[16] Shao, J., Wu, L., Wu, J., Zheng, Y., Zhao, H., Jin, Q., Zhao, J., *Lab Chip* 2009, *9*, 3118–3125.

[17] Chin, L. K., Yu, J. Q., Fu, Y., Yu, T., Liu, A. Q., Luo, K. Q., *Lab Chip* 2011, *11*, 1856–1863.

[18] Song, J. W., Gu, W., Futai, N., Warner, K. A., Nor, J. E., Takayama, S., *Anal. Chem.* 2005, *77*, 3993–3999.

[19] Nalayanda, D. D., Puleo, C. M., Fulton, W. B., Wang, T. H., Abdullah, F., *Exp. Lung Res.* 2007, *33*, 321–335.

[20] Nalayanda, D. D., Wang, Q., Fulton, W. B., Wang, T.-H., Abdullah, F., *J. Pediatr. Surg.* 2010, *45*, 45–51.

[21] Esch, M. B., Post, D. J., Shuler, M. L., Stokol, T., *Tissue Eng. A* 2011, *17*, 2965–2971.

[22] Huh, D., Matthews, B. D., Mammoto, A., Montoya-Zavala, M., Hsin, H. Y., Ingber, D. E., *Science* 2010, *328*, 1662–1668.

[23] Young, E. W. K., Watson, M. W. L., Srigunapalan, S., Wheeler, A. R., Simmons, C. A., *Anal. Chem.* 2010, *82*, 808–816.

[24] Douville, N. J., Tung, Y.-C., Li, R., Wang, J. D., El-Sayed, M. E. H., Takayama, S., *Anal. Chem.* 2010, *82*, 2505–2511.

[25] Vogel, P. A., Halpin, S. T., Martin, R. S., Spence, D. M., *Anal. Chem.* 2011, *83*, 4296–4301.

[26] Leclerc, E., David, B., Griscom, L., Lepioufle, B., Fujii, T., Layrolle, P., Legallaisa, C., *Biomaterials* 2006, *27*, 586–595.

[27] Kou, S., Pan, L., van Noort, D., Meng, G., Wu, X., Sun, H., Xu, J., Lee, I., *Biochem. Biophys. Res. Commun.* 2011, *408*, 350–355.

[28] Sato, K., Mawatari, K., Kitamori, T., *Lab Chip* 2008, *8*, 1992–1998.

[29] Tanaka, Y., Kikukawa, Y., Sato, K., Sugii, Y., Kitamori, T., *Anal. Sci.* 2007, *23*, 261–266.

[30] Yamashita, T., Tanaka, Y., Idota, N., Sato, K., Mawatari, K., Kitamori, T., *Biomaterials* 2011, *32*, 2459–2465.

[31] Jang, K., Sato, K., Igawa, K., Chung, U.-I., Kitamori, T., *Anal. Bioanal. Chem.* 2008, *390*, 825–832.

[32] Herricks, T., Seydel, K. B., Turner, G., Molyneux, M., Heyderman, R., Taylor, T., Rathod, P. K., *Lab Chip* 2011, *11*, 2994–3000.

[33] Bowen, A. L., Martin, R. S., *Electrophoresis* 2010, *31*, 2534–2540.

[34] Gómez-Sjöberg, R., Leyrat, A. A., Pirone, D. M., Chen, C. S., Quake, S. R., *Anal. Chem.* 2007, *79*, 8557–8563.

[35] Futai, N., Gu, W., Song, J. W., Takayama, S., *Lab Chip* 2006, *6*, 149–154.

[36] Ades, E. W., Candal, F. J., Swerlick, R. A., George, V. G., Summers, S., Bosse, D. C., Lawley, T. J., *J. Invest. Dermatol.* 1992, *99*, 683–690.

[37] Hosokawa, K., Fujii, T., Endo, I., *Anal. Chem.* 1999, *71*, 4781–4785.

[38] Imura, Y., Asano, Y., Sato, K., Yoshimura, E., *Anal. Sci.* 2009, *25*, 1403–1407.

[39] Hosokawa, K., Sato, K., Ichikawa, N., Maeda, M., *Lab Chip* 2004, *4*, 181–185.

[40] Young, E. W., Simmons, C. A., *Lab Chip* 2010, *10*, 143–160.

[41] Morita, K., Sasaki, H., Furuse, M., Tsukita, S., *J. Cell Biol.* 1999, *147*, 185–194.

[42] Tarbell, J. M., *Cardiovasc. Res.* 2010, *87*, 320–330.

[43] Rodewald, M., Herr, D., Duncan, W. C., Fraser, H. M., Hack, G., Konrad, R., Gagsteiger, F., Kreienberg, R., Wulff, C., *Human Reprod.* 2009, *24*, 1191–1199.

[44] Beese, M., Wyss, K., Haubitz, M., Kirsch, T., *BMC Cell Biol.* 2010, *11*, 68.

Included in the theme issue:
SKIN ONCOLOGY SPECIAL
Acta Derm Venereol 2012; 92: 585–663

Twist1 as a Possible Biomarker for Metastatic Basal Cell Carcinoma

Yuta Majima[1], Satoshi Hirakawa[1]*, Yukiko Kito[1], Hiroki Suzuki[1], Masayo Koide[2], Hidekazu Fukamizu[3] and Yoshiki Tokura[1]
*Departments of [1]Dermatology and [3]Plastic and Reconstructive Surgery, Hamamatsu University School of Medicine, Hamamatsu 431-3192, and [2]Division of Dermatology, Hamamatsu Red Cross Hospital, Hamamatsu 434-8533, Japan. *E-mail: hirakawa@hama-med.ac.jp*
Accepted May 8, 2012.

Basal cell carcinoma (BCC), a common tumour of epithelial origin, is locally invasive and has a low risk of metastasis, estimated to range from 0.028% to 0.1% (1). However, once BCC metastasizes to distant organs, the effective therapeutic options are limited, leading to poor patient outcome.

Recent studies have shown that epithelial-mesenchymal transition (EMT) suppresses epithelial features, and induces mesenchymal traits to epithelial cells in several pathological conditions (2, 3). Of note is that tumours of epithelial origin can express transcription factors Snail and Twist1, or the cell adhesion molecule N-cadherin as a mesenchymal marker. We have previously shown that N-cadherin is up-regulated in invasive tumours, but not in carcinoma *in situ* of extramammary Paget's disease, and that EMT is associated with distant organ metastasis, leading to poor patient survival (4, 5). However, it remains unclear whether EMT plays a key role in the development of highly invasive phenotype and potential metastasis in BCC. We report here the first case of morphoeic and metastatic BCC showing the induction of Twist1 and the epithelial-to-mesenchymal conversion of cadherins in association with multiple organ metastases.

CASE REPORT

A 51-year-old Japanese man presented with a 3-cm ulcerated nodule with peripheral focal pigmentation on the upper back (Fig. 1a). A biopsy specimen disclosed the proliferation and invasion of epithelial strands with mesenchymal transition and rich stroma, indicating a diagnosis of morphoeic BCC (Fig. 1b). The patient underwent a tumour resection, and the defect was reconstructed with the trapezius musculocutaneous flap. After 4 years of follow-up, a subcutaneous mass appeared in the patient's supraclavicular fossa. Under the histological diagnosis of metastatic BCC, the tumour was surgically resected with subsequent reconstruction using the pectoral major musculo-cutaneous flap, followed by a total of 60 Gy radiation to the local region. However, multiple foci of tumour metastasis were found in the left levator scapulae muscle and the pleura of the left lung by magnetic resonance imaging. The patient underwent systemic chemotherapy with a combination of cisplatin and doxorubicin. However, the therapeutic effect was minimal, and at the time of writing, the tumours were disseminated in the lung.

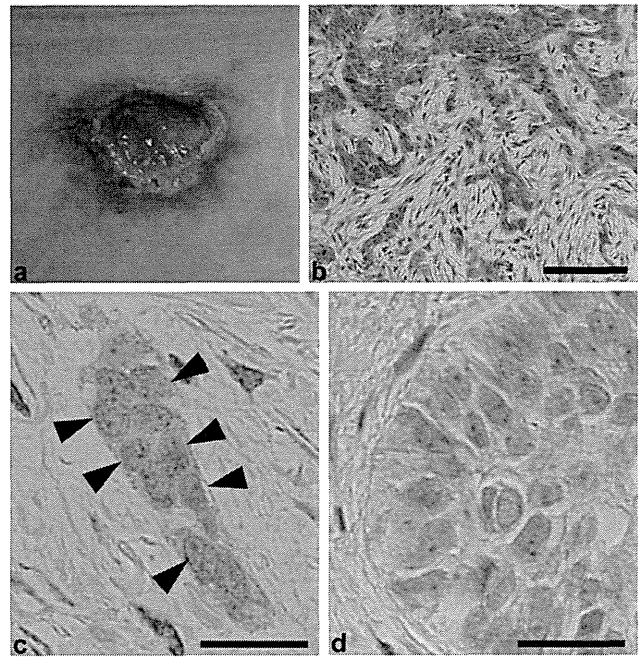

Fig. 1. Clinical, roentgenological, and pathological features in metastatic basal cell carcinoma (BCC). (a) Clinical presentation of 3-cm ulcerated nodule on the upper back with peripheral, focal pigmentation. (b) Haematoxylin & eosin stains (×400) of the cutaneous primary site show foci of basaloid tumour cells on the superiorly and infiltrative tumour cells within the stroma. (c) Prominent Twist1 expression was revealed in the nuclei of tumour cells (*arrowheads*) at the invasive front in the index case. (d) No Twist1 expression was found in control representative nodular BCC by immunohistochemistry. Scale bars = 100 μm (b); 30 μm (c, d).

To clarify the potential role of EMT in metastatic BCC, we investigated the tumour by immunohistochemical analyses. Formalin-fixed paraffin-embedded sections of the index case showed that the tumour cells were positive for Twist1 at the invasive front of the primary tumour (Fig. 1c), whereas the tumour cells centrally were negative for Twist1. In order to specify Twist1 expression in metastatic BCC, control representative tumour cells of nodular BCC were analysed by immunohistochemistry (Fig. 1d). These non-metastatic tumour cells showed no Twist1 expression in the nuclei (Fig. 1d). Furthermore, double immunofluorescence stains for E-cadherin and N-cadherin showed that E-cadherin was prominently expressed in the nodular form of BCC (Fig. 2a), whereas this epithelial marker was markedly decreased in the tumour cells of the index case (Fig. 2b). In contrast, whereas no N-cadherin expression was found in the control nodular form of BCC (Fig. 2c), tumour cells of the index case markedly bore N-cadherin

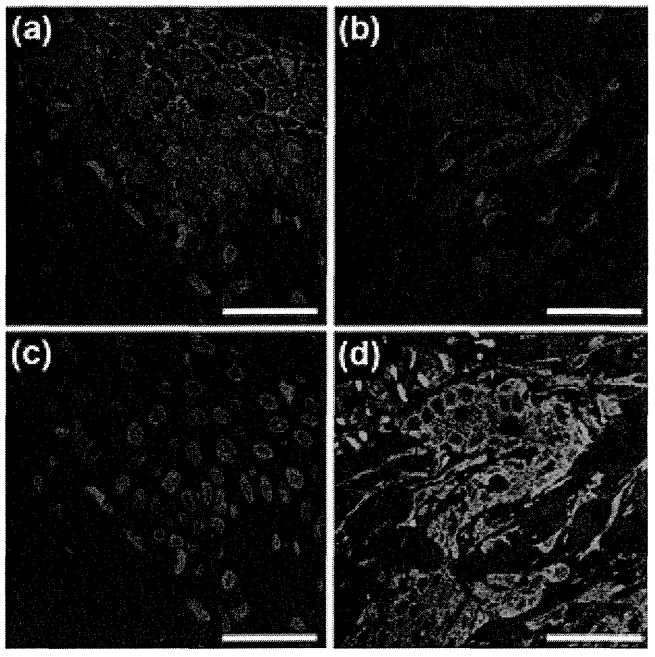

Fig. 2. Cadherin conversion by epithelial-mesenchymal transition (EMT) in metastatic basal cell carcinoma (BCC). Double immunofluorescence stains for E-cadherin (*red*) and N-cadherin (*green*) in non-metastatic nodular BCC as control (a, c) and the index case (b, d). E-cadherin was prominently expressed by tumour cells in nodular BCC (a), whereas no N-cadherin was observed in those cells (c). In contrast, the expression levels of E-cadherin were markedly decreased in tumour cells at the invasive front in the index case (b). Furthermore, N-cadherin was strikingly induced in those cells (d), indicating that highly invasive and metastatic BCC is capable of converting epithelial characteristics to mesenchymal features by EMT. Nuclei are stained in blue with 4',6-diamidino-2-phenylindole. (a–d) Scale bars = 50 μm.

at the invasive front (Fig. 2d). Moreover, high levels of expression of Twist1 and N-cadherin were found in metastatic tumour cells of the supraclavicular fossa in the index case, whereas E-cadherin expression was markedly decreased in the metastatic tumours. Therefore, these results demonstrate, for the first time, that highly invasive and metastatic BCC may show Twist1 expression and an epithelial-to-mesenchymal conversion of cadherins in the primary sites, indicating that EMT might play a key role in the promotion of tumour invasion and subsequent metastasis.

DISCUSSION

The present case reveals a potential impact of Twist1 on marked invasion and metastasis in BCC. Twist1, a basic helix-loop-helix transcription factor, was originally identified as a master regulator of EMT and metastasis in an experimental tumour model (6). Furthermore, Twist1 is significantly up-regulated in patients with metastatic breast cancer compared with those who remained at early stages (7). Twist1 may be a feasible biomarker for highly invasive and/or metastatic BCC. The expression levels of Snail, the other transcription factor promoting EMT, have been shown to correlate with the depth of tumour invasion in BCC (8). However, no significant relationship was found between Snail and down-regulation of E-cadherin (8), suggesting that another transcription factor is involved in the regulation of EMT in BCC. Our finding is in accordance with the notion that Twist1 is capable of promoting EMT, contributing to aggressive invasion and multiple organ metastases.

The primary tumour of the present patient was histopathologically diagnosed as morphoeic BCC, a stroma-rich form of the cutaneous neoplasm. We previously showed that EMT markers Snail and Twist1 were expressed in the eccrine glands in patients with systemic sclerosis (2, 9). Therefore, a subpopulation of cell lineages in eccrine glands might undergo EMT and further differentiate into the myofibroblasts, contributing to marked fibrosis of the disease. In the present case, tumour cells prominently expressed Twist1 at the invasive front, forming morphoeic fibrosis within the primary sites. Of note, tissue fibrosis is mediated by several inflammatory cytokines, such as transforming growth factor-β, which is a key soluble factor facilitating EMT in tumour progression. Thus, BCC undergoing EMT might induce fibrotic skin change, and subsequently develop tumour cell invasion and metastasis.

REFERENCES

1. Kirkham N. Tumors and cysts of the epidermis. In: Elder DE, editor. Lever's histopathology of the skin. 9th edn. Philadelphia: Lippincott Williams & Wilkins, 2005, p. 805–866.
2. Nakamura M, Tokura Y. Epithelial-mesenchymal transition in the skin. J Dermatol Sci 2011; 61: 7–13.
3. Kalluri R, Weinberg RA. The basics of epithelial-mesenchymal transition. J Clin Invest 2009; 119: 1420–1428.
4. Hirakawa S, Tanemura A, Mori H, Katayama I, Hashimoto K. Multiple lymphadenopathy as an initial sign of extramammary Paget's disease. Br J Dermatol 2011; 164: 200–203.
5. Hirakawa S, Detmar M, Kerjaschki D, Nagamatsu S, Matsuo K, Tanemura A, et al. Nodal lymphangiogenesis and metastasis: Role of tumor-induced lymphatic vessel activation in extramammary Paget's disease. Am J Pathol 2009; 175: 2235–2248.
6. Yang J, Mani SA, Donaher JL, Ramaswamy S, Itzykson RA, Come C, et al. Twist, a master regulator of morphogenesis, plays an essential role in tumor metastasis. Cell 2004; 117: 927–939.
7. Kallergi G, Papadaki MA, Politaki E, Mavroudis D, Georgoulias V, Agelaki S. Epithelial to mesenchymal transition markers expressed in circulating tumor cells of early and metastatic breast cancer patients. Breast Cancer Res 2011; 13: R59.
8. Papanikolaou S, Bravou V, Gyftopoulos K, Nakas D, Repanti M, Papadaki H. ILK expression in human basal cell carcinoma correlates with epithelial-mesenchymal transition markers and tumor invasion. Histopathology 2010; 56: 799–809.
9. Nakamura M, Tokura Y. Expression of SNAI1 and TWIST1 in the eccrine glands of patients with systemic sclerosis: possible involvement of epithelial-mesenchymal transition in the pathogenesis. Br J Dermatol 2011; 164: 204–205.

J. Biochem. 2013;153(1):5–11 doi:10.1093/jb/mvs128

JB THE JOURNAL OF BIOCHEMISTRY

JB Review

The vasohibin family: a novel family for angiogenesis regulation

Received August 28, 2012; accepted September 24, 2012; published online October 25, 2012

Yasufumi Sato*

Department of Vascular Biology, Institute of Development, Aging and Cancer, Tohoku University, 4-1 Seiryo-machi, Aoba-ku, Sendai 980-8575, Japan

*Yasufumi Sato, Department of Vascular Biology, Institute of Development, Aging and Cancer, Tohoku University, 4-1 Seiryo-machi, Aoba-ku, Sendai 980-8575, Japan.
Tel: +81-22-717-8528, Fax: +81-22-717-8533,
email: y-sato@idac.tohoku.ac.jp

Angiogenesis, a formation of neovessels, is regulated by the local balance between angiogenesis stimulators and inhibitors. A number of such endogenous regulators of angiogenesis have been found in the body. Recently, vasohibin-1 (VASH1) was isolated as a negative feedback regulator of angiogenesis produced by endothelial cells (ECs) and subsequently vasohibin-2 (VASH2) as a homologue of VASH1. It was then explored that VASH1 is expressed in ECs to terminate angiogenesis, whereas VASH2 is expressed in cells other than ECs to promote angiogenesis in the mouse model of angiogenesis. This review will focus on the vasohibin family members, which are novel regulators of angiogenesis.

Keywords: angiogenesis/endothelial cell/SVBP/vasohibin-1/vasohibin-2.

Abbreviations: EC, endothelial cell; FGF-2, fibroblast growth factor 2; KO, knockout; MNC, mononuclear cell; SVBP, small vasohibin-binding protein; VASH1, vasohibin-1; VASH2, vasohibin-2; VEGF, vascular endothelial growth factor; VEGFR, vascular endothelial growth factor receptor.

The vasculature is primarily composed of luminal endothelial cells (ECs) and surrounding mural cells (smooth muscle cells or pericytes). ECs are multifunctional cells covering the entire luminal surface of all blood vessels. ECs remain G_0 phase of the cell cycle and form an interface between the circulating blood between the lumen and the rest of the vessel wall, and maintain vascular homeostasis. Physiological function of ECs includes the transport of various molecules across the vascular wall, the regulation of the adhesion of leukocytes for extravasation, the manipulation of vascular tonus and the prevention of thrombotic events. However, when stimulated by angiogenic factors, ECs migrate, proliferate and form neovessels for angiogenesis. The initial step of angiogenesis is the extrication of mural cells from endothelial tubes for vascular destabilization. Subsequently, specialized ECs, the so-called tip cells, migrate by extending numerous filopodia, whereas following ECs, the so-called stalk cells, proliferate causing elongation of the sprouts to form immature tube-like structures. Finally, redistributed mural cells affix themselves to the newly formed vessels for vascular restabilization. By this process, ECs stop their proliferation, thus terminating angiogenesis (*1*).

The body contains a number of endogenous angiogenesis stimulators and inhibitors, and the local balance between them regulates this process of blood vessel formation. Angiogenesis stimulators are mostly growth factors and cytokines including vascular endothelial growth factor (VEGF), whereas angiogenesis inhibitors are variable and include hormones, chemokines, proteins accumulated in the extracellular matrix, proteolytic fragments of various proteins and so forth. In addition, the majority of angiogenesis inhibitors are extrinsic to the vasculature; some are constitutively expressed and act as barriers to prevent the invasion of sprouts, and the others are generated in response to stimuli and counteract this process (*2*).

Isolation of VASH1 and VASH2

It could be hypothesized that ECs themselves might produce either angiogenesis stimulators or inhibitors as an autoregulatory or a feedback fashion. To test this hypothesis, cDNA microarray analysis was performed to detect VEGF-inducible genes in ECs (*3*). Among a variety of VEGF-inducible genes, an attention was focused on genes whose functions were undefined. *In vitro* functional assays for angiogenesis were performed, and one gene having anti-angiogenic activity was isolated. This gene was designated as *vasohibin-1* (*VASH1*), and its *in vivo* anti-angiogenic activity was further confirmed (*4*). The gene for human *VASH1* gene is located on chromosome 14q24.3 and consists of seven exons (Fig. 1). There are two isoforms of human VASH1: full-length VASH1A and the spliced variant VASH1B (Fig. 1). Human VASH1A protein is composed of 365 amino acid residues, whereas human VASH1B protein is composed of 204 amino acid residues, and this splicing variant maintains anti-angiogenic activity (*5*, *6*).

By searching in the database, one gene homologous to VASH1 was found and designated as *vasohibin-2* (*VASH2*) (*7*). The gene for human *VASH2* is located on chromosome 1q32.3. So far, nine exons for the *VASH2* gene have been shown in the database to form multiple transcripts owing to alternative splicing (Fig. 1). The full-length human VASH2 was found to be expressed in cultured cells, which is composed of 355 amino acid residues (*7*). The overall homology between full-length human VASH1 and VASH2 is 52.5% at the amino acid level.

The phylogenic tree of vasohibin family proteins reveals that parasite or sea squirt possesses one common

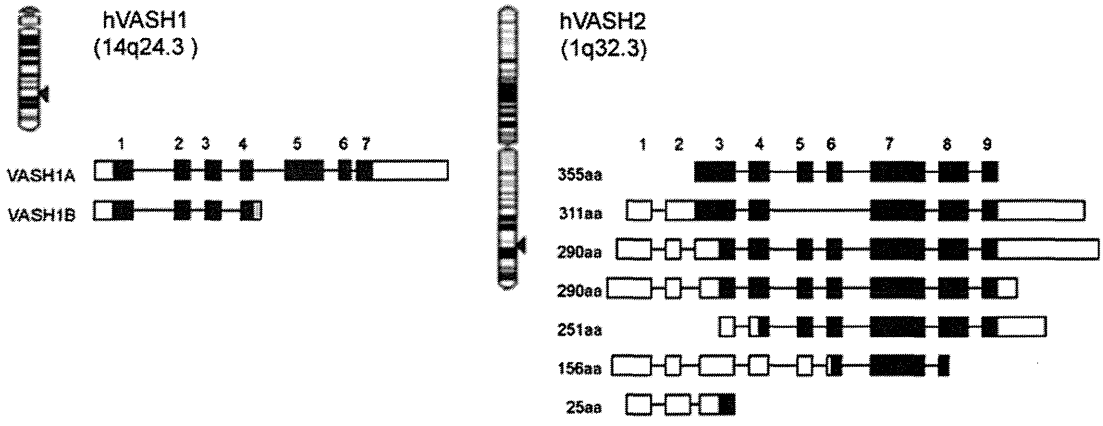

Fig. 1 ***VASH1* and *VASH2* genes and their transcripts.** Human *VASH1* gene is encoded in 14q24.3, whereas human *VASH2* gene is encoded in 1q32.3. There are multiple transcripts in both human *VASH1* and *VASH2*. Black squares indicate encode proteins.

ancestry vasohibin gene, while vertebrates have *VASH1* and *VASH2* (Fig. 2). The homology between sea squirt vasohibin and human VASH1 or human VASH2 is about 40%. Moreover, amino acid sequences of vertebrate VASH1 and VASH2 are well conserved. Thus, a common ancestry gene seems to be divided into VASH1 and VASH2 during the evolution to vertebrate. No known functional motifs were found in the amino acid sequences in either VASH1 or VASH2. This makes extremely difficult to estimate the functions and compare three-dimensional structures of these two molecules. Instead, the order/disorder orientation of VASH1 and VASH2 proteins estimated by Protein Disorder Prediction System (http://prdos.hgc.jp/cgi-bin/top.cgi) would provide useful information. The order region defines stable in a three-dimensional composition, whereas the disorder region defines unstable in a three-dimensional composition. In addition, the disorder region is more important for determining the function of proteins. As shown in Fig. 3, VASH1 and VASH2 contain disorder regions in both N-terminus and C-terminus ends and order region in the centre. The overall order/disorder probability lines of VASH1 and VASH2 are considerably resemble, indicating the correspondence of these two molecules. However, when similarity of order and disorder area was compared, disorder areas are less resemble (Fig. 3). The differences in the disorder regions may indicate the distinctive function of VASH1 and VASH2.

Isolation of Small Vasohibin-Binding Protein

To understand the undefined characteristics of vasohibins, their possible binding partners were searched by using a yeast two-hybrid technique, and one candidate gene was discovered (*8*). This gene was registered in the database as hypothetical protein LOC374969 or coiled-coil domain containing 23. The binding of this protein to VASH1 and VASH2 was confirmed by using the BIAcore system. Because this protein is composed of 66 amino acids, this molecule was renamed as small vasohibin-binding protein (SVBP) (*8*). The database search revealed that SVBP is highly conserved between species. The analysis of the function of SVBP revealed that SVBP binds to vasohibins within the cells, makes a heterodimer with vasohibins and facilitates the secretion of vasohibins. The knockdown of SVBP impedes the secretion of vasohibins, and vasohibins remained in the cells are degraded via the proteasome–ubiquitin system (*8*). Because vasohibins lack classical signal sequence for secretion, it has been obscure whether vasohibins are secreted. The isolation of SVBP verifies vasohibins as secretory proteins, and SVBP acts as a secretory chaperone of vasohibins.

Expression and Function of VASH1 and VASH2

As one can see from its discovery, the expression of VASH1 in ECs is inducible. The VEGF receptor (VEGFR)-induced expression of VASH1 in ECs is mediated via VEGFR2 and its downstream PKCδ (*5*). VASH1 is induced not only by VEGF but also by fibroblast growth factor 2, another potent angiogenic factor (*4*, *5*), and this induction is also mediated by PKCδ (*5*). Accordingly, the principal signalling pathways for the induction of VASH1 by these two representative angiogenic growth factors considerably overlap. Interestingly, this induction of VASH1 in ECs disappears under a hypoxic condition or in the presence of inflammatory cytokines, tumour necrosis factor-α and interleukin-1 (*5*).

In contrast, the expression of VASH2 seems to be not inducible but constitutive as it is not modulated by growth factors and cytokines. In connection with this expression pattern of VASH2, recently, VASH2 is found as the target of mir-200 (*9*). There is a cluster of miR-200bc/429 binding sites in the 3' untranslated region of VASH2 mRNA, and mir-200b silences the expression of VASH2. Thus, the expression of VASH2 is augmented when the expression of mir-200b declines (*9*).

Large collections of microarray data contain information about concerted changes in transcript levels in the datasets beyond the original purpose of each dataset, and the co-expressed gene database (http://

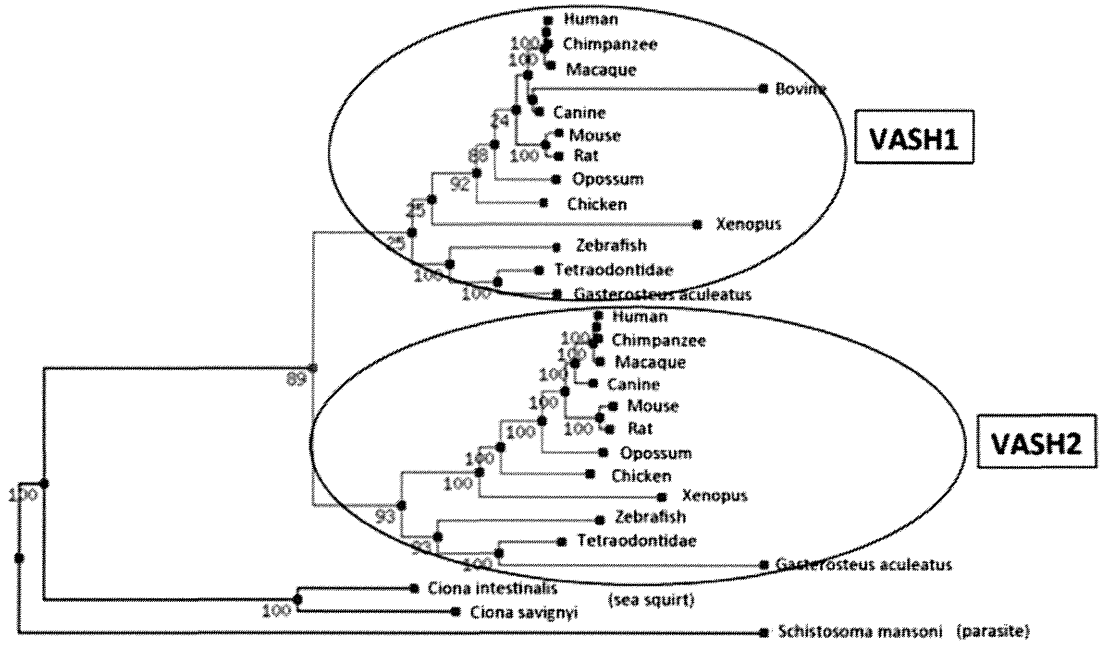

Fig. 2 The phylogenic tree of vasohibin family proteins. Parasite and sea squirt have one vasohibin ancestry gene, whereas vertebrates have *VASH1* and *VASH2*. A common ancestry gene seems to be divided into *VASH1* and *VASH2* during the evolution to vertebrate.

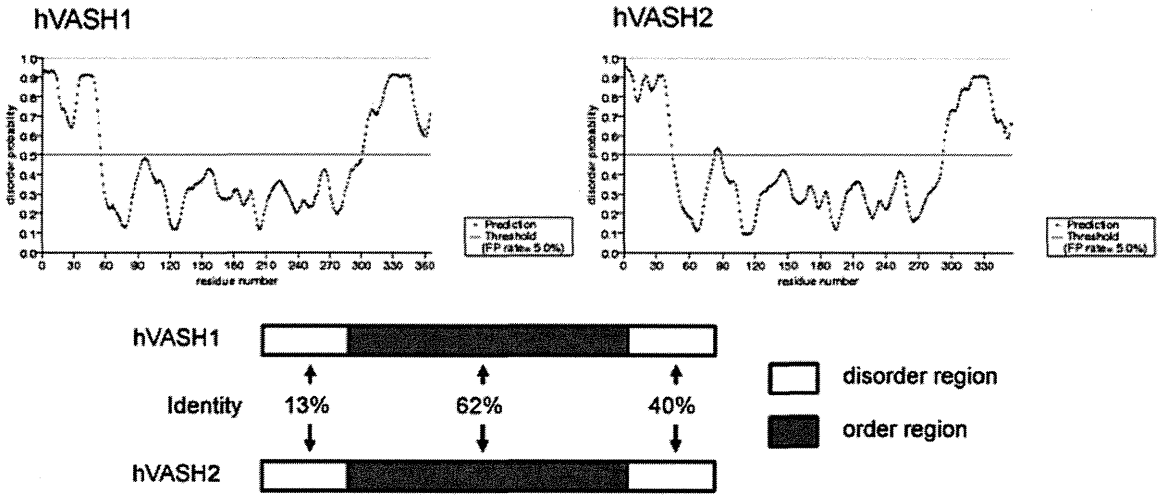

Fig. 3 Order/disorder configuration of human VASH1 and VASH2 proteins. Order/disorder probability lines of human VASH1 and human VASH2 are shown on the top. Area above the line of disorder probability 0.5 is regarded as disorder region. Similarities of order and disorder regions are shown at the bottom.

coxpresdb.jp/) using those datasets will determine the co-expressed genes with *VASH1* and *VASH2* are compared by the use of this database, and the results revealed that co-expressed genes with VASH1 and VASH2 are completely different (Fig. 4). This information may suggest that the cells expressing VASH1 and VASH2 are different.

To disclose the precise relationship of VASH1 and VASH2, their spatiotemporal expression and function during angiogenesis were examined (*10*). The analysis using the mouse subcutaneous angiogenesis model revealed that VASH1 is expressed not in ECs at the sprouting front but in newly formed blood vessels behind the sprouting front where angiogenesis terminates. In contrast, VASH2 is expressed preferentially in mononuclear cells (MNCs) that are mobilized from the bone marrow and infiltrate the sprouting front. *VASH1* and *VASH2* knockout (KO) mice were generated and used in this analysis. *VASH1* KO mice contain numerous immature microvessels in the area where angiogenesis should be terminated. This phenotype was gene dosage sensitive, as more enhanced angiogenesis was observed in *VASH1* (−/−) mice (*10*). Importantly, newly formed immature microvessels in *VASH1* (−/−) mice are functional, as indicated by blood flow (*10*). In contrast, *VASH2* KO mice

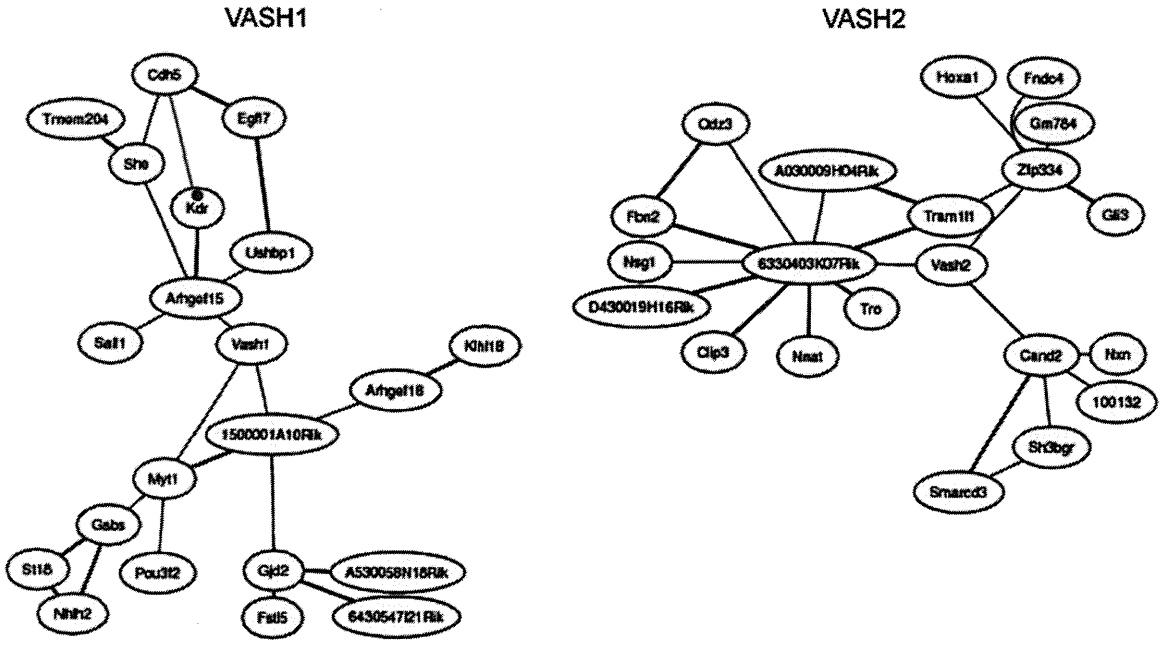

Fig. 4 Co-expressed genes with VASH1 and VASH2. Co-expressed genes with VASH1 are shown on the left and those with VASH2 are on the left.

contain less neovessels in the sprouting front of angiogenesis. This phenotype was also gene dosage sensitive, as more impaired angiogenesis was observed in *VASH2* (−/−) mice (*10*). Importantly, the infiltration of MNCs in *VASH2* (−/−) mice is identical to that of wild-type mice (*10*). As described earlier, the expression of VASH1 is low in proliferating ECs at the sprouting front but high in non-proliferating ECs (*10*). In addition, angiogenesis in the *VASH2* KO mice was deficient at the sprouting front (*10*). These results indicate that VASH1 is expressed in ECs in the termination zone of angiogenesis to terminate angiogenesis, whereas VASH2 is mainly expressed in MNCs in the sprouting front and promotes angiogenesis (Fig. 5).

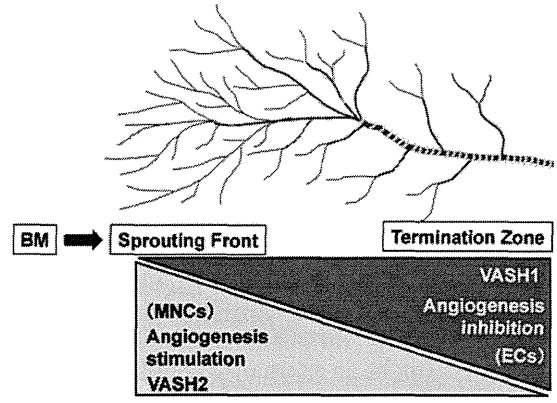

Fig. 5 Spacial expression and function of VASH1 and VASH2 in the regulation of angiogenesis. VASH1 is mainly expressed in ECs at the termination zone and halts angiogenesis. In contrast, VASH2 is mainly expressed in MNCs at the sprouting front mobilized from bone marrow (BM) and promotes angiogenesis.

VASH1 and VASH2 in Pathophysiology

Immunohistochemical analysis has revealed that VASH1 protein is present in ECs in the developing human or mouse embryo, but it is reduced in expression in the post-neonate (*7*). Nimmagadda *et al.* independently showed by *in situ* hybridization that VASH1 mRNA is expressed in a wide range of tissues and organs in the chicken embryo and suggested that the expression of VASH1 might not be limited to ECs (*11*). Indeed, VASH1 mRNA was detected in bone marrow hematopoietic stem cells (*12*) and striated muscles (*13*). Although the significance of these expression is not clear (*14*), immunohistochemical analysis preferentially detects VASH1 protein in ECs at the site of angiogenesis (*4*, *7*). The expression of VASH1 was further investigated under various conditions accompanied by pathological angiogenesis and a related condition. The presence of VASH1 in ECs is evident in various cancers, atherosclerotic lesions, age-dependent macular degeneration, diabetic retinopathy, rheumatoid arthritis and arterial re-endothelialization after denudation (*15–27*). Even under pathological conditions, the extent of angiogenesis may vary. Tumours inoculated into *VASH1* (−/−) mice contain numerous immature vessels, resulting in a growth advantage of the tumours (*20*). These observations suggest that VASH1 should regulate the course of angiogenesis under pathological conditions as well. Interestingly, Lu *et al.* recently reported that EZH2 silenced the VASH1 expression in ovarian cancers and that made the prognosis of ovarian cancers worse (*28*).

The initial analysis on VASH2 revealed that VASH2 protein was also present in ECs in the developing human or mouse embryo and faded in the

post-neonate (*7*). However, when the expression of VASH2 was examined in postnatal angiogenesis, it was shown not in ECs but in infiltrating MNCs (*10*). The analysis was extended to pathological conditions including cancers thereafter and showed the expression of VASH2 in cancer cells of gastric cancer (*29*), hepatocellular carcinoma (*30*) and ovarian serous adenocarcinoma (*9*). This increased expression of VASH2 in cancer cells can be mediated by modulating the methylation of its promoter region (*27*) or the decrease of mir-200b (*9*). Importantly, the knockdown of VASH2 expression in cancer cells prominently inhibited both tumour growth and tumour angiogenesis (*9*, *27*). These results indicate that VASH2 is expressed in cancer cells and promotes tumour growth by stimulating angiogenesis.

Therapeutic Application of Vasohibin

Because of the anti-angiogenic potential, VASH1 can be applied to treat diseases associated with angiogenesis. Its efficacy in anti-angiogenic treatment has been reported in animal models of cancers, ocular (retinal or choroidal) angiogenesis, arterial intimal stenosis, diabetic nephropathy and pulmonary diseases such as pulmonary fibrosis and bronchiolitis obliterans (*4*, *14*, *19*, *31–41*).

Anti-angiogenic drugs that are now available in the clinics target VEGF-mediated signals. Those drugs are used for the treatment of cancers and age-related macular degeneration, but have some problems. Because VEGF acts as survival factor of ECs, such drugs cause cardiovascular toxicities including hypertension and proteinuria due to the impairment of normal ECs (*42*). However, VASH1 does not cause hypertension and proteinuria (*43*). Another problem is drug resistance due to the switch from VEGF to other angiogenic stimulators (*44*). As VASH1 inhibits not only VEGF-induced angiogenesis but also angiogenesis induced by various angiogenesis stimulators (*34*), VASH1 can be an alternative option for the treatment of pathological angiogenesis.

Because of the broad-spectrum anti-angiogenic activity of VASH1, the possible effect of VASH1 on lymphangiogenesis was examined (*34*). Peripheral lymphatic vessels are composed of a single layer of lymphatic ECs without mural cell coverage, and their function is to collect fluid lost from blood vessels and to maintain immune responses, lipid uptake and tissue homeostasis. Recently, attention has focused on lymphangiogenesis, because it has been shown to be related to lymph node (LN) metastasis of cancers. Angiogenesis is counter balanced by various endogenous inhibitors. However, little is known about endogenous inhibitors of lymphangiogenesis. The effect of VASH1 in the corneal micropocket assay was carefully examined, and it revealed broad-spectrum anti-angiogenic and anti-lymphangiogenic activities of VASH1 (*34*). In addition, VASH1 inhibited tumour lymphangiogenesis and tumour LN metastasis (*34*). Accordingly, VASH1 is the first molecule intrinsic to the endothelium that exhibits anti-lymphangiogenic activities.

Concluding Remarks

This study has focused on the VASH family members, VASH1 and VASH2. VASH1 and VASH2 are highly conserved between species, and their roles in the regulation of angiogenesis are distinct and perhaps contradictory. VASH1 is mainly expressed in ECs for the termination of angiogenesis, whereas VASH2 is expressed in infiltrating MNCs or cancer cells to stimulate angiogenesis. It has been recently described that VASH1 induces prolyl hydroxylase–mediated degradation of hypoxia-inducible factor-1α in human umbilical vein ECs (*45*). However, its significance on the effect of VASH1 is unclear. Apparently, further studies including their receptor and its downstream signalling are required to disclose the entire function of these unique family proteins.

Funding
This author is supported by a grant from the program Grant-in-Aid for Scientific Research on Priority Areas from the Japanese Ministry of Education, Science, Sports and Culture; Health and Labour Sciences research grants (22112006); Third Term Comprehensive Control Research for Cancer (H22-3-008); Japanese Ministry of Health, Labour, and Welfare (22300323).

Conflict of interest
None declared.

References

1. Carmeliet, P. and Jain, R.K. (2011) Molecular mechanisms and clinical applications of angiogenesis. *Nature* **473**, 298–307
2. Sato, Y. (2006) Update on endogenous inhibitors of angiogenesis. *Endothelium* **13**, 147–155
3. Abe, M. and Sato, Y. (2001) cDNA microarray analysis of the gene expression profile of VEGF-induced human umbilical vein endothelial cells. *Angiogenesis* **4**, 289–298
4. Watanabe, K., Hasegawa, Y., Yamashita, H., Shimizu, K., Ding, Y., Abe, M., Ohta, H., Imagawa, K., Hojo, K., Maki, H., Sonoda, H., and Sato, Y. (2004) Vasohibin as an endothelium-derived negative feedback regulator of angiogenesis. *J. Clin. Invest.* **114**, 898–907
5. Shimizu, K., Watanabe, K., Yamashita, H., Abe, M., Yoshimatsu, H., Ohta, H., Sonoda, H., and Sato, Y. (2005) Gene regulation of a novel angiogenesis inhibitor, vasohibin, in endothelial cells. *Biochem. Biophys. Res. Commun.* **327**, 700–706
6. Kern, J., Bauer, M., Rychli, K., Wojta, J., Ritsch, A., Gastl, G., Gunsilius, E., and Untergasser, G. (2008) Alternative splicing of vasohibin-1 generates an inhibitor of endothelial cell proliferation, migration, and capillary tube formation. *Arterioscler. Thromb. Vasc. Biol.* **28**, 478–484
7. Shibuya, T., Watanabe, K., Yamashita, H., Shimizu, K., Miyashita, H., Abe, M., Moriya, T., Ohta, H., Sonoda, H., Shimosegawa, T., Tabayashi, K., and Sato, Y. (2006) Isolation and characterization of vasohibin-2 as a homologue of VEGF-inducible endothelium-derived angiogenesis inhibitor vasohibin. *Arterioscler. Thromb. Vasc. Biol.* **26**, 1051–1057
8. Suzuki, Y., Kobayashi, M., Miyashita, H., Ohta, H., Sonoda, H., and Sato, Y. (2010) Isolation of a small

vasohibin-binding protein (SVBP) and its role in vasohibin secretion. *J. Cell Sci.* **123**, 3094–4101

9. Takahashi, Y., Koyanagi, T., Suzuki, Y., Saga, Y., Kanomata, N., Moriya, T., Suzuki, M., and Sato, Y. (2012) Vasohibin-2 expressed in human serous ovarian adenocarcinoma accelerates tumor growth by promoting angiogenesis. *Mol. Cancer Res.* **10**, 1135–1146
10. Kimura, H., Miyashita, H., Suzuki, Y., Kobayashi, M., Watanabe, K., Sonoda, H., Ohta, H., Fujiwara, T., Shimosegawa, T., and Sato, Y. (2010) Distinctive localization and opposed roles of vasohibin-1 and vasohibin-2 in the regulation of angiogenesis. *Blood* **113**, 4810–4818
11. Nimmagadda, S., Geetha-Loganathan, P., Pröls, F., Scaal, M., Christ, B., and Huang, R. (2007) Expression pattern of vasohibin during chick development. *Dev. Dyn.* **236**, 1358–1362
12. Naito, H., Kidoya, H., Sato, Y., and Takakura, N. (2009) Induction and expression of anti-angiogenic vasohibins in the hematopoietic stem/progenitor cell population. *J. Biochem.* **145**, 653–659
13. Kishlyansky, M., Vojnovic, J., Roudier, E., Gineste, C., Decary, S., Forn, P., Bergeron, R., Desplanches, D., and Birot, O. (2010) Striated muscle angio-adaptation requires changes in vasohibin-1 expression pattern. *Biochem. Biophys. Res. Commun.* **399**, 359–364
14. Sato, Y. (2011) Is vasohibin-1 for more than angiogenesis inhibition? *J. Biochem.* **149**, 229–230
15. Yamashita, H., Abe, M., Watanabe, K., Shimizu, K., Moriya, T., Sato, A., Satomi, S., Ohta, H., Sonoda, H., and Sato, Y. (2006) Vasohibin prevents arterial neointimal formation through angiogenesis inhibition. *Biochem. Biophys. Res. Commun.* **345**, 919–925
16. Yoshinaga, K., Ito, K., Moriya, T., Nagase, S., Takano, T., Niikura, H., Yaegashi, N., and Sato, Y. (2008) Expression of vasohibin as a novel endothelium-derived angiogenesis inhibitor in endometrial cancer. *Cancer Sci.* **99**, 914–919
17. Wakusawa, R., Abe, T., Sato, H., Yoshida, M., Kunikata, H., Sato, Y., and Nishida, K. (2008) Expression of vasohibin, an antiangiogenic factor, in human choroidal neovascular membranes. *Am. J. Ophthalmol.* **146**, 235–243
18. Tamaki, K., Moriya, T., Sato, Y., Ishida, T., Maruo, Y., Yoshinaga, K., Ohuchi, N., and Sasano, H. (2008) Vasohibin-1 in human breast carcinoma: a potential negative feedback regulator of angiogenesis. *Cancer Sci.* **100**, 88–94
19. Sato, H., Abe, T., Wakusawa, R., Asai, N., Kunikata, H., Ohta, H., Sonoda, H., Sato, Y., and Nishida, K. (2009) Vitreous levels of vasohibin-1 and vascular endothelial growth factor in patients with proliferative diabetic retinopathy. *Diabetologia* **52**, 359–361
20. Hosaka, T., Kimura, H., Heishi, T., Suzuki, Y., Miyashita, H., Ohta, H., Sonoda, H., Moriya, T., Suzuki, S., Kondo, T., and Sato, Y. (2009) Vasohibin-1 expressed in endothelium of tumor vessels regulates angiogenesis. *Am. J. Pathol.* **175**, 430–439
21. Miyake, K., Nishida, K., Kadota, Y., Yamasaki, H., Nasu, T., Saitou, D., Tanabe, K., Sonoda, H., Sato, Y., Maeshima, Y., and Makino, H. (2009) Inflammatory cytokine-induced expression of vasohibin-1 by rheumatoid synovial fibroblasts. *Acta Med. Okayama* **63**, 349–358
22. Tamaki, K., Sasano, H., Maruo, Y., Takahashi, Y., Miyashita, M., Moriya, T., Sato, Y., Hirakawa, H., Tamaki, N., Watanabe, M., Ishida, T., and Ohuchi, N. (2010) Vasohibin-1 as a potential predictor of aggressive behavior of ductal carcinoma in situ of the breast. *Cancer Sci.* **101**, 1051–1058
23. Yoshinaga, K., Ito, K., Moriya, T., Nagase, S., Takano, T., Niikura, H., Sasano, H., Yaegashi, N., and Sato, Y. (2011) Roles of intrinsic angiogenesis inhibitor, vasohibin, in cervical carcinomas. *Cancer Sci.* **102**, 446–451
24. Miyazaki, Y., Kosaka, T., Mikami, S., Kikuchi, E., Tanaka, N., Maeda, T., Ishida, M., Miyajima, A., Nakagawa, K., Okada, Y., Sato, Y., and Oya, M. (2012) The prognostic significance of vasohibin-1 expression in patients with upper urinary tract urothelial carcinoma. *Clin. Cancer Res.* **18**, 4145–4153
25. Wang, Q., Tian, X., Zhang, C., and Wang, Q. (2012) Upregulation of vasohibin-1 expression with angiogenesis and poor prognosis of hepatocellular carcinoma after curative surgery. *Med. Oncol.* **29**, 2727–2736
26. Zhao, G., Yang, Y., Tang, Y., Han, R., and Sun, Y. (2012) Reduced expression of vasohibin-1 is associated with clinicopathological features in renal cell carcinoma. *Med. Oncol.*, PMID: 22865127 [Epub ahead of print]
27. Bai, X., Margariti, A., Hu, Y., Sato, Y., Zeng, L., Ivetic, A., Habi, O., Mason, J.C., Wang, X., and Xu, Q. (2010) PKCδ-deficiency accelerates neointimal lesion of mouse injured artery involving delayed reendothelialization and vasohibin-1 accumulation. *Arterioscler. Thromb. Vasc. Biol.* **30**, 2467–2474
28. Lu, C., Han, H.D., Mangala, L.S., Ali-Fehmi, R., Newton, C.S., Ozbun, L., Armaiz-Pena, G.N., Hu, W., Stone, R.L., Munkarah, A., Ravoori, M.K., Shahzad, M.M., Lee, J.W., Mora, E., Langley, R.R., Carroll, A.R., Matsuo, K., Spannuth, W.A., Schmandt, R., Jennings, N.B., Goodman, B.W., Jaffe, R.B., Nick, A.M., Kim, H.S., Guven, E.O., Chen, Y.H., Li, L.Y., Hsu, M.C., Coleman, R.L., Calin, G.A., Denkbas, E.B., Lim, J.Y., Lee, J.S., Kundra, V., Birrer, M.J., Hung, M.C., Lopez-Berestein, G., and Sood, A.K. (2010) Regulation of tumor angiogenesis by EZH2. *Cancer Cell* **18**, 185–197
29. Shen, Z., Kauttu, T., Seppänen, H., Vainionpää, S., Ye, Y., Wang, S., Mustonen, H., and Puolakkainen, P. (2012) Vasohibin-1 and vasohibin-2 expression in gastric cancer cells and TAMs. *Med. Oncol.* **29**, 2718–2726
30. Xue, X., Gao, W., Sun, B., Xu, Y., Han, B., Wang, F., Zhang, Y., Sun, J., Wei, J., Lu, Z., Zhu, Y., Sato, Y., Sekido, Y., Miao, Y., and Kondo, Y. (2012) Vasohibin 2 is transcriptionally activated and promotes angiogenesis in hepatocellular carcinoma. *Oncogene*, 2012 [Epub ahead of print; doi:10.1038/onc.2012.177]
31. Shen, J., Yang, X., Xiao, W.H., Hackett, S.F., Sato, Y., and Campochiaro, P.A. (2006) Vasohibin is up-regulated by VEGF in the retina and suppresses VEGF receptor 2 and retinal neovascularization. *FASEB J.* **20**, 723–725
32. Nasu, T., Maeshima, Y., Kinomura, M., Hirokoshi-Kawahara, K., Tanabe, K., Sugiyama, H., Sonoda, H., Sato, Y., and Makino, H. (2009) Vasohibin-1, a negative feedback regulator of angiogenesis, ameliorates renal alterations in a mouse model of diabetic nephropathy. *Diabetes* **58**, 2365–2375
33. Li, D., Zhou, K., Wang, S., Shi, Z., and Yang, Z. (2010) Recombinant adenovirus encoding vasohibin prevents tumor angiogenesis and inhibits tumor growth. *Cancer Sci.* **101**, 448–452
34. Heishi, T., Hosaka, T., Suzuki, Y., Miyashita, H., Oike, Y., Takahashi, T., Nakamura, T., Arioka, S., Mitsuda, Y., Takakura, T., Hojo, K., Matsumoto, M., Yamauchi, C., Ohta, H., Sonoda, H., and Sato, Y. (2010) Endogenous angiogenesis inhibitor vasohibin1 exhibits

a broad-spectrum anti-lymphangiogenic activity and suppresses lymph node metastasis. *Am. J. Pathol.* **176**, 1950–1958

35. Wang, X., Zhu, H., Yang, X., Bi, Y., and Cui, S. (2010) Vasohibin attenuates bleomycin induced pulmonary fibrosis via inhibition of angiogenesis in mice. *Pathology* **42**, 457–462
36. Zhou, S.Y., Xie, Z.L., Xiao, O., Yang, X.R., Heng, B.C., and Sato, Y. (2010) Inhibition of mouse alkali burn induced-corneal neovascularization by recombinant adenovirus encoding human vasohibin-1. *Mol. Vis.* **16**, 1389–1398
37. Saito, D., Maeshima, Y., Nasu, T., Yamasaki, H., Tanabe, K., Sugiyama, H., Sonoda, H., Sato, Y., and Makino, H. (2011) Amelioration of renal alterations in obese type 2 diabetic mice by vasohibin-1, a negative feedback regulator of angiogenesis. *Am. J. Physiol. Renal Physiol.* **300**, F873–F886
38. Wakusawa, R., Abe, T., Sato, H., Sonoda, H., Sato, M., Mitsuda, Y., Takakura, T., Fukushima, T., Onami, H., Nagai, N., Ishikawa, Y., Nishida, K., and Sato, Y. (2011) Suppression of choroidal neovascularization by vasohibin-1, a vascular endothelium-derived angiogenic inhibitor. *Invest. Ophthalmol. Vis. Sci.* **52**, 3272–3280
39. Onami, H., Nagai, N., Machida, S., Kumasaka, N., Wakusawa, R., Ishikawa, Y., Sonoda, H., Sato, Y., and Abe, T. (2012) Reduction of laser-induced choroidal neovascularization by intravitreal vasohibin-1 in monkey eyes. *Retina* **32**, 1204–1213
40. Chen, H., Fan, K., Wang, S., Liu, Z., and Zheng, Z. (2012) Dual targeting of glioma U251 cells with nanoparticles prevents tumor angiogenesis and inhibits tumor growth. *Curr. Neurovasc. Res.* **9**, 133–138
41. Watanabe, T., Okada, Y., Hoshikawa, Y., Eba, S., Notsuda, H., Watanabe, Y., Ohishi, H., Sato, Y., and Kondo, T. (2012) A potent anti-angiogenic factor, vasohibin-1, ameliorates experimental bronchiolitis obliterans. *Transplant. Proc.* **44**, 1155–1157
42. des Guetz, G., Uzzan, B., Chouahnia, K., and Morère, J.F. (2011) Cardiovascular toxicity of anti-angiogenic drugs. *Target Oncol.* **6**, 197–202
43. Miyashita, H., Suzuki, H., Ohkuchi, A., and Sato, Y. (2011) Mutual balance between vasohibin-1 and soluble VEGFR-1 in endothelial cells. *Pharmaceuticals* **4**, 1551–1577
44. Bergers, G. and Hanahan, D. (2008) Modes of resistance to anti-angiogenic therapy. *Nat. Rev. Cancer* **8**, 592–603
45. Kozako, T., Matsumoto, N., Kuramoto, Y., Sakata, A., Motonagare, R., Aikawa, A., Imoto, M., Toda, A., Honda, S., Shimeno, H., and Soeda, S. (2012) Vasohibin induces prolyl hydroxylase-mediated degradation of hypoxia-inducible factor-1α in human umbilical vein endothelial cells. *FEBS Lett.* **586**, 1067–1072

Oncogene (2013) 32, 1724–1734

www.nature.com/onc

ORIGINAL ARTICLE

Vasohibin 2 is transcriptionally activated and promotes angiogenesis in hepatocellular carcinoma

X Xue[1,5], W Gao[1,5], B Sun[1], Y Xu[1], B Han[2], F Wang[1], Y Zhang[1], J Sun[1], J Wei[1], Z Lu[1], Y Zhu[1], Y Sato[3], Y Sekido[4], Y Miao[1] and Y Kondo[4]

Hepatocellular carcinoma (HCC) typically relies on angiogenesis for its malignant behavior, including growth and metastasis. Vasohibin 2 (VASH2) was previously identified as an angiogenic factor, but its role in tumorigenesis is unknown. Using quantitative PCR and western blot analyses, we found that *VASH2* is overexpressed in HCC cells and tissues. Using chromatin immunoprecipitation, we detected histone modifications at the putative *VASH2* promoter, with increased H3K4 trimethylation and H3 acetylation and decreased H3K27 trimethylation, suggesting that epigenetic mechanisms are responsible for the deregulated *VASH2* transcription in HCC. Knockdown of *VASH2* via siRNA inhibited the proliferation of the hepatoma cell lines by delaying cell cycle progression and increasing apoptosis. Importantly, we found VASH2 secreted in the culture supernatant, and co-expression of its secretory chaperone small vasohibin-binding protein (SVBP) further enhanced VASH2 secretion. The supernatant from HepG2 cells expressing VASH2 enhanced the proliferation, migration and tube formation of human umbilical vein endothelial cells, and knockdown of *VASH2* significantly inhibited these effects. In an *in vivo* study using a nude mouse model, we found that exogenous VASH2 significantly contributed to tumor growth, microvessel density and hemoglobin concentration in the tumors. Further analyses showed that the VASH2-mediated increase in the transcription of fibroblast growth factor-2, vascular endothelial growth factor and vasohibin 1 may be the mechanism underlying these effects. Taken together, these data indicate that VASH2 is abnormally expressed in HCC cells as a result of histone modifications and that VASH2 contributes to the angiogenesis in HCC via an SVBP-mediated paracrine mechanism. These results indicate a novel and important role for VASH2 in HCC angiogenesis and malignant transformation.

Oncogene (2013) **32,** 1724–1734; doi:10.1038/onc.2012.177; published online 21 May 2012

Keywords: angiogenesis; vasohibin 2; hepatocellular carcinoma; histone modification

INTRODUCTION

Hepatocellular carcinoma (HCC) is the fifth most common tumor type worldwide and the third most common cause of cancer-related deaths. However, systemic chemotherapy is not effective for the treatment of HCC. HCC typically relies on angiogenesis for its malignant behavior, including tumor growth and metastasis, and because HCC is vascularized, chemoembolization improves the survival of patients with advanced HCC. Therefore, targeting angiogenesis seems to be a promising approach for the treatment of HCC.[1] Vascular endothelial growth factor (VEGF)[2–4] is an important angiogenic factor in the hypoxic conditions associated with tumors, and anti-angiogenic agents that inhibit the VEGF pathway have been approved for the treatment of HCC (for example, Sorafenib for advanced HCC[5]). Unfortunately, less than half of all patients with advanced HCC benefit from these therapies, and these benefits are often only transient.[6] Therefore, the identification of targets other than VEGF is important for clarifying the mechanisms underlying angiogenesis in HCC and testing future therapeutic strategies.[7]

Vasohibin 2 (VASH2) belongs to the VASH family, which includes vasohibin 1 (VASH1) and VASH2. VASH1 is selectively induced in endothelial cells (ECs) by angiogenic factors, such as VEGF, and operates as an intrinsic and highly specific feedback inhibitor of activated ECs engaged in angiogenesis.[8] Recently, VASH1 was found to be involved in angiogenesis in various solid tumors, and exogenous VASH1 significantly blocks sprouting angiogenesis by tumors.[9,10] *VASH2* was first described by Shibuya *et al.*[11] In contrast with VASH1, VASH2 has been found to promote angiogenesis.[12]

Unlike VEGF and other angiogenic factors, VASH2 has been identified as an extrinsic and VEGF-independent angiogenic factor that is highly expressed in bone marrow-derived mononuclear cells but weakly expressed in ECs. Although its role in tumor angiogenesis is unknown, it is likely that VASH2 functions via mechanisms that are distinct from those of VEGF, which may make it a novel target for tumor therapy.

In this study, we show that *VASH2* transcription is upregulated in HCC cells via an epigenetic mechanism, and this increased expression contributes to HCC angiogenesis through paracrine effects. This study identifies a new and important role for VASH2 in HCC angiogenesis and malignant transformation and suggests that VASH2 may be a novel target for the treatment of HCC and other malignancies.

[1]Department of General Surgery, the First Affiliated Hospital with Nanjing Medical University, Nanjing, China; [2]Department of Endocrinology, Nanjing Children's Hospital Affiliated to Nanjing Medical University, Nanjing, China; [3]Department of Vascular Biology, Institute of Development, Aging and Cancer, Tohoku University, 4-1 Seiryo-machi, Aoba-ku, Sendai, Japan and [4]Division of Molecular Oncology, Aichi Cancer Center Research Institute, 1-1 Kanokoden, Chikusa-Ku, Nagoya, Japan. Correspondence: Y Miao or W Gao, Department of General Surgery, the First Affiliated Hospital with Nanjing Medical University, 300# GuangZhou Road, Nanjing 210029, China or Y Kondo, Division of Molecular Oncology, Aichi Cancer Center Research Institute, 1-1 Kanokoden, Chikusa-ku, Nagoya 464-8681, Japan.
E-mail: miaoyi@njmu.edu.cn or gao11@hotmail.com or ykondo@aichi-cc.jp
[5]These authors contributed equally to this work.
Received 17 November 2011; revised 28 March 2012; accepted 9 April 2012; published online 21 May 2012

RESULTS

Increased VASH2 expression in HCC cells and tissue

We used a Taqman quantitative reverse transcription (qRT)–PCR-based strategy to measure *VASH2* expression in three HCC cell lines, the normal liver cell line L02 and human umbilical vein ECs (HUVECs). As observed in Figure 1a, qPCR showed HepG2 cells expressed *VASH2* at higher levels than normal L02 cells or HUVECs ($P<0.05$). HUVECs had a low level of *VASH2* expression, similar to the results reported by Shibuya *et al.*[11] Beside, western blot coincided with qPCR results except L02 showed no band and HUVECs showed very low VASH2 expression. To confirm the expression level of *VASH2* in tissues, we also measured *VASH2* expression in 5 normal liver tissue samples and in 65 HCC tissue samples with paired adjacent non-cancerous tissue using qRT–PCR. *VASH2* expression in the normal liver tissue samples was very low but was slightly higher in the tissue adjacent to HCC tumors and significantly higher in the HCC tumors themselves. Of the 65 paired samples, 44 showed significantly higher *VASH2* expression in the cancer tissue compared with the adjacent tissue (Figure 1b, $P<0.05$). The same trend can be observed using a scatter plot (Figure 1c), which shows that the mean expression level of *VASH2* in tumors, tumor-adjacent normal tissue and normal liver was 47.89, 12.47 and 1.54, respectively. Beside, we detected VASH2 in clinical samples with immunohistochemistry. The result (Figure 1d) showed VASH2 had a high expression in the tumor cells of HCC sample and almost no expression in the normal liver tissue. From the Figure 1d, we could see that VASH2 was located in the plasma of tumor cells. Taken together, our results show that VASH2 is highly expressed in HCC cells and tissue, indicating that VASH2 might be activated during tumorigenesis and have an important role in HCC.

Histone modifications at the putative core promoter contribute to the activation of VASH2 transcription

Histone modifications at promoters can form a histone code that tightly regulates gene expression.[13,14] H3K4 trimethylation (H3K4triMe) and H3 acetylation (H3Ac) are associated with active transcription, whereas H3K27 trimethylation (H3K27triMe) is correlated with transcriptional repression.[15–17] As histone modifications have been shown to be an important epigenetic mechanism underlying the deregulation of cancer-related gene expression in tumors, we investigated whether the increased

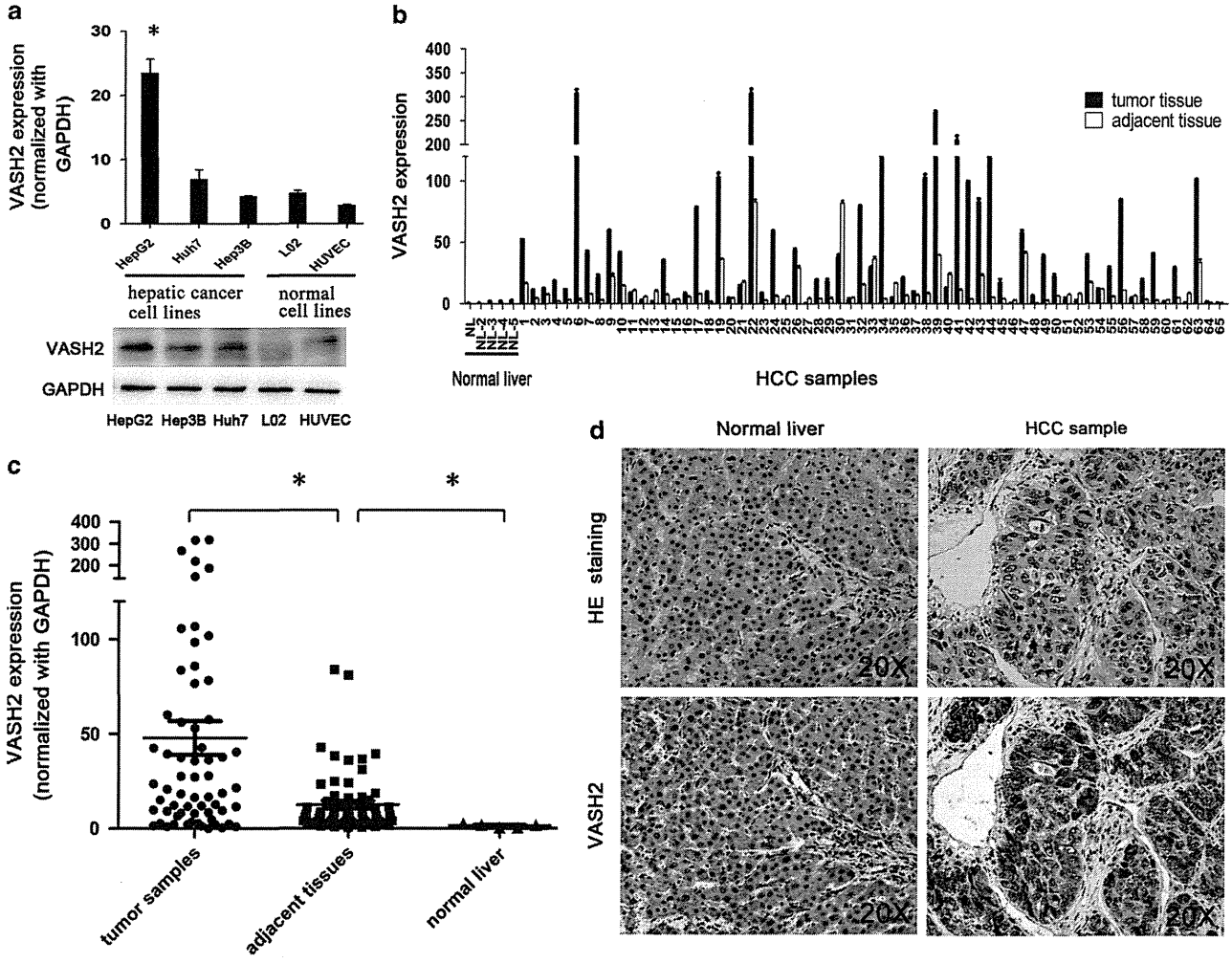

Figure 1. *VASH2* expression in cell lines and tissues. (**a**) qRT–PCR and western blot analysis of *VASH2* expression in HCC cell lines, the normal liver cell line L02 and HUVECs. HepG2 cells showed higher expression of *VASH2* than other cell lines ($P<0.05$). (**b**) *VASH2* expression in 5 normal liver tissues and 65 pairs of hepatic cancer tissue and adjacent tissue. Normal liver tissues had very low expression of *VASH2*, whereas the non-cancerous tissue adjacent to tumors had slightly higher expression, and hepatic cancer tissues showed the highest level of expression. Of the 65 pairs of tissues, *VASH2* expression was greater in the cancer tissue than in the adjacent tissues in 44 cases ($P<0.05$). (**c**) A scatter plot showing the results of *VASH2* expression in the same cancer tissue, adjacent tissue and normal liver samples (mean expression: 47.89, 12.47 and 1.54, respectively). (**d**) Immunohistochemistry showed VASH2 location in the clinical HCC sample. Magnification, ×20 (*represents $P<0.05$ when compared to the control group).

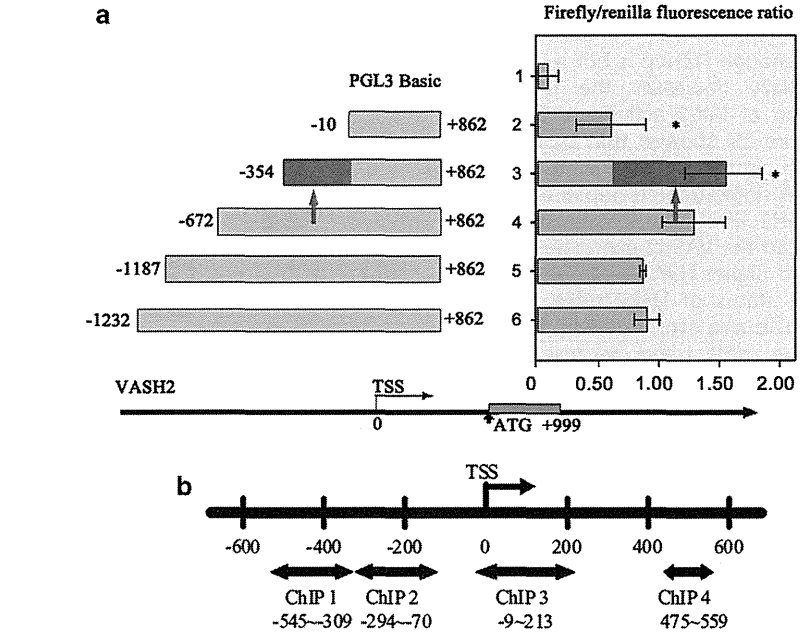

c

Primers	Forward	Reverse
ChIP 1	CTCAACTTGGGCTTAAAGGG	TTTGGCATCAGAAGAGCATT
ChIP 2	GGGGTCACTTCTCGGGTGGT	CCGCGACGCTCTGATTGG
ChIP 3	GACGCATTCGGAACATC	CAGCTCCAAGATCCTACC
ChIP 4	GGACCCAGGAATGTGTGGA	CGCAAGATGTGGGGAGAAG

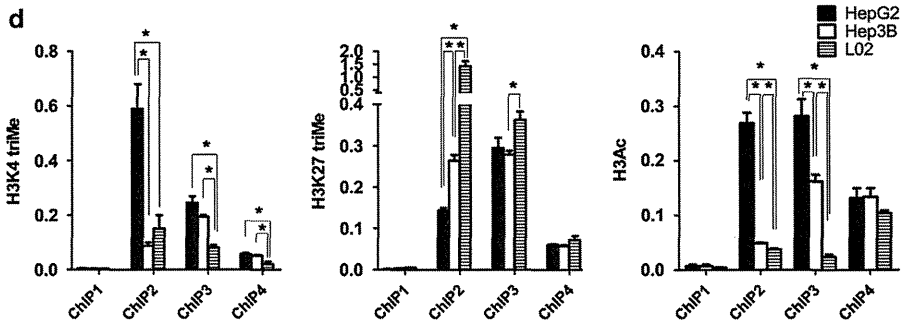

Figure 2. Histone modification in putative promoter of *VASH2*. (**a**) Dual luciferase reporter assay. Different segments flanking the TSS of the *VASH2* gene were amplified and ligated into the pGL3 basic vector. The plasmids were co-transfected with a *Renilla* luciferase expression plasmid into HepG2 cells, and luciferase activity was measured. The region from − 354 to + 862 had the strongest promoter activity, and the region from − 352 to − 10 seemed to be the key part (the red arrow indicates the position; $^*P<0.05$ when compared with the control group transfected with the pGL3 basic vector). The TSS was defined to be position 0. (**b**) Map of the four real-time–PCR amplicons (ChIP 1–ChIP 4) used to analyze *VASH2* promoters by ChIP. ChIP-2 (amplifies − 294 to − 70) overlaps with the core promoter region (− 352 to − 10). (**c**) The primer sequences used to analyze the four regions of *VASH2* usingChIP. (**d**) HepG2 cells have increased levels of H3K4triMe and H3Ac and decreased levels of H3K27triMe at the *VASH2* promoter compared with Hep3B and L02 cells, while L02 showed silent histone code. The data are presented as the average of three independent experiments with the s.e. ($^*P<0.05$ between the indicated groups). No enrichment of these four amplicons was observed in control immunoglobulin G immunoprecipitations (data not shown). A full color version of this figure is available at the *Oncogene* journal online.

expression of *VASH2* in our HCC cell lines was associated with aberrant histone modifications.

To test this, we first analyzed the putative promoter region of *VASH2* (− 1232 to + 862, flanking the transcriptional start site (TSS)) using a luciferase reporter assay. As observed in Figure 2a, the region from − 354 to + 862 had the strongest promoter activity, and the region from − 354 to − 10 seemed to be the core part accounting for increasing promoter activity ($P<0.05$).

Next, we performed chromatin immunoprecipitation (ChIP) to compare the histone modifications around the *VASH2* promoter region in two HCC cell lines and the normal liver cells L02, HepG2 (high *VASH2* expression) and Hep3B or L02(low *VASH2* expression). The amplicon sizes with four primer sets are shown in Figures 2b and c. Histone-associated DNA fragments immunoprecipitated with antibodies against H3K4triMe, H3K27triMe and H3Ac were analyzed using PCR with primers designed to amplify different regions of the *VASH2* promoter. Interestingly, the region amplified using the ChIP-2 primer set, which spans the core promoter identified in the reporter assay, had a more active histone code in HepG2 cells, which have high *VASH2* expression, than the histone code in Hep3B and L02 cells, which have low *VASH2* expression. Specifically, increased H3K4triMe and H3Ac modifications and decreased H3K27triMe modifications were found; no such code was found in other examined regions (Figure 2d).

To further confirm the ChIP result, we used the 3-deazaneplanocin A (DZnep) and trichostatin A (TSA) to treat the above three cells. TSA could increase H3Ac. Although DZNep is not a specific inhibitor of EZH2, it preferentially decreases the level of H3K27me3 through the disruption of PRC2 activity. qPCR and western blot (Supplementary Figure 2S) showed that DZnep- or TSA-single-treated HepG2 had no significant change in VASH2 expression, whereas DZnep- or TSA-single-treated Hep3B and L02 had an obvious increase in VASH2 level. The combination of DZnep and TSA treatment increased the VASH2 expression in all three cells. As Hep3B and L02 had higher H3K27triMe, therefore DZnep treatment decreased the status of H3K27triMe, which recovered the VASH2 expression. This also explained why DZnep-treated HepG2 did not show the same trend because lower H3K27triMe.

These results clearly indicate that histone modifications associated with transcriptional activation were observed at the putative core promoter in HCC cell lines with high VASH2 expression, suggesting that aberrant epigenetic modifications are responsible for the increased VASH2 expression in HCC cells.

Generation and identification of stably transfected cells

To further address the functions of VASH2 in HCC, we overexpressed and silenced *VASH2* expression. HepG2 cells with higher level of VASH2 and Hep3B with lower level of VASH2 were chosen for these experiments. We constructed *VASH2* overexpression and *VASH2*-knockout lentiviral constructs, infected HepG2 cells and selected stably infected cells. We confirmed the expression levels using qRT–PCR and western blot (Figure 3). Stable cells of Hep3B were treated the same as HepG2 (Data were not shown).

VASH2 promotes proliferation of HepG2 cells *in vitro*

The growth of the stable cell lines over 5 days was determined using 3-(4,5-dimethythiazol-2-yl)-2,5-diphenyl tetrazolium bromide assay. As shown in Figure 4a, *VASH2* knockdown significantly impaired the proliferation of cells after day 3 ($P<0.05$). To further study the mechanism by which *VASH2* knockdown affected proliferation, cell cycle progression and apoptosis were analyzed using flow cytometry. G2 + S% phase reflects cell proliferation ability. *VASH2*-knockout cells showed a delayed G2 and S phase compared with the wild-type HepG2 cells (49.9% ± 2.1% vs 40.7% ± 1.0%) (Figure 4b, $P<0.05$). In addition, *VASH2* silencing increased the frequency of apoptosis of HepG2-shVASH2 cells (17.1% ± 1.2%) when compared with wild-type HepG2 cells (12.3% ± 1.0%; Figure 4c, $P<0.05$). Therefore, *VASH2* knockdown inhibited the proliferation of HepG2 cells via a delay in cell cycle progression and increased apoptosis. We got the same result in Hep3B(Supplementary Figure 4S). These results suggest a role for *VASH2* in the positive regulation of HCC cell proliferation.

Small vasohibin-binding protein (SVBP) facilitates VASH2 secretion by functioning as a chaperone in HCC

As VASH2 was identified as an angiogenic factor,[12] we hypothesized that VASH2 overexpression in HCC cells could contribute to angiogenesis in HCC, possibly via secretion from HCC cells and action on ECs in a paracrine manner. Although a previous study showed that VASH2 and VASH1 lack the classic signal sequence required for secretion, a small protein known as SVBP has been shown to aid in the secretion of VASH2.[18] As such, we constructed an SVBP-expressing lentivirus and infected HepG2-VASH2 and Hep3B-VASH2 cells (to generate HepG2-VASH2-SVBP and Hep3B-VASH2-SVBP, respectively). qPCR and western blot (SVBP was fused with V5 tag) showed that SVBP was overexpressed >50-fold (Figure 5a), and overexpression of either SVBP or VASH2 did not alter the endogenous transcription of the other gene (data not shown). Supernatants were collected from

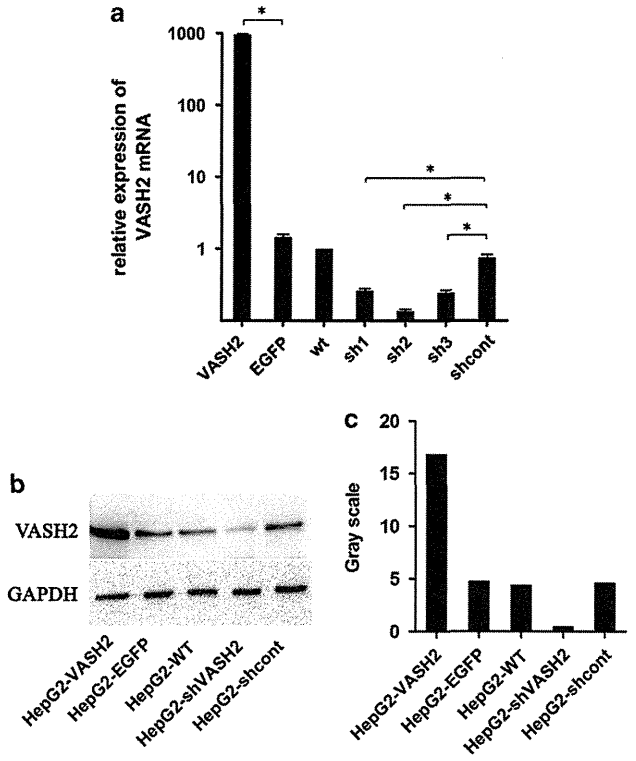

Figure 3. Generation and identification of stably transfected HepG2 cells. (**a**) Measurement of *VASH2* expression using qRT–PCR. VASH2 indicates VASH2-overexpressing HepG2 cells; EGFP indicates HepG2 cells transfected with a vector-expressing EGFP. Wt indicates wild-type HepG2 cells. The cells transduced with the three shRNAs and one control shRNA are designated as 'sh1', 'sh2', 'sh3' and 'shcont'. VASH2-overexpressing HepG2 cells showed almost 1000-fold higher *VASH2* expression than wild-type HepG2 cells, whereas VASH2-knockdown HepG2 cells had 80% lower expression when compared with wild-type HepG2 cells (*$P<0.05$ compared with the corresponding control group). (**b**) Western blots were used to confirm the efficiency of knockdown. The results are similar to those seen in the qRT–PCR analyses. (**c**) Gray scale analysis of the western blot data.

HepG2-VASH2-SVBP and HepG2-VASH2 cells after 24, 48 and 72 h of culture, and an enzyme-linked immunosorbent assay with VASH2 monoclonal antibody was used to quantify VASH2 secretion into the supernatant. VASH2 secretion from HepG2-VASH2-SVBP cells was significantly higher than that from HepG2-VASH2 cells, and the level in the supernatant increased with time (Figure 5b), similar to previously reported results.[18] Beside, we got the same results in Hep3B cells (data not shown). Following co-expression of SVBP, VASH2 secretion increased significantly, indicating that SVBP facilitates VASH2 secretion by functioning as a chaperone.

VASH2 promotes migration and angiogenesis of HUVECs *in vitro* in a paracrine manner

Following the confirmation of VASH2 secretion by HCC cells, its direct effect on ECs was analyzed. First, we collected supernatants from cultures of HepG2-VASH2-SVBP, HepG2-VASH2, HepG2-wt, HepG2-shVASH2 and HepG2-shcont cells after 48 h of culture, and the conditioned medium (CM) was added to adherent HUVECs. Seventy-two hours after the addition of the CM, 3-(4,5-dimethythiazol-2-yl)-2,5-diphenyl tetrazolium assays were performed to measure HUVEC proliferation. The HepG2-VASH2-SVBP CM caused the nost proliferation than HepG2-VASH2 and HepG2-wt CM, whereas the HepG2-shVASH2 CM caused less proliferation

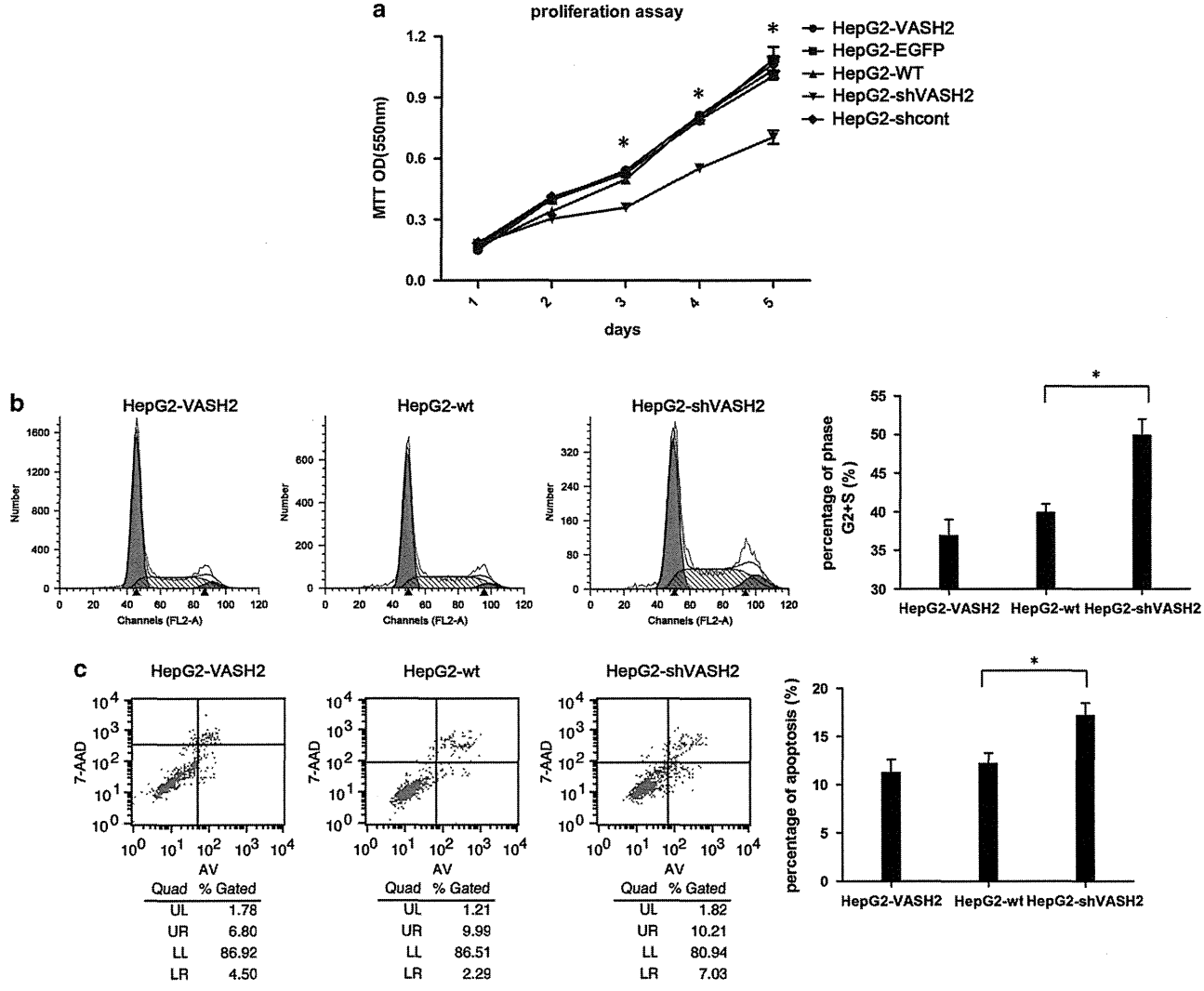

Figure 4. Effects of VASH2 on the proliferation of HepG2 cells. (**a**) The growth of cells over 5 days was measured using 3-(4,5-dimethythiazol-2-yl)-2,5-diphenyl tetrazolium bromide (MTT) assays. The proliferation rate of HepG2-shVASH2 cells was significantly decreased compared with HepG2-wt cells. $^*P<0.05$. (**b**) Cell cycle progression was measured using flow cytometry. The progression of HepG2-shVASH2 cells was delayed in the G2 and S phase compared with HepG2-wt and HepG2-VASH2 cells. The percentage of cells in the G2 and S phase was HepG2-VASH2, 37.2 ± 2.0%; HepG2-wt, 40.7% ± 1.0%; and HepG2-shVASH2, 49.9% ± 2.1%. (**c**) Apoptosis was measured using flow cytometry. The HepG2-shVASH2 cells had a higher apoptosis rate than the HepG2-VASH2 or HepG2-wt cells. ($^*P<0.05$ compared with HepG2-wt cells). A full color version of this figure is available at the *Oncogene* journal online.

than the HepG2-shcont CM (Figure 6a, $P<0.05$). This result indicates that VASH2 promotes the proliferation of HUVECs and that the different levels of VASH2 secreted into the supernatant caused different rates of proliferation.

Next, we confirmed the effect of the CM on the migration of HUVECs using transwell chambers. The HepG2-VASH2-SVBP CM had a significantly greater ability to promote the migration of HUVECs than the HepG2-VASH2 and HepG2-wt CM, whereas the HepG2-shVASH2 CM showed less migration of HUVECs than the control group (Figures 6b and d, $P<0.05$), and the HepG2-VASH2 CM did not enhance migration compared with HepG2-wt CM.

In addition, we performed tube formation assays with the CM. We found that the HepG2-shVASH2 CM failed to promote complete network formation, whereas the HepG2-VASH2-SVBP CM promoted the most network formation than HepG2-VASH2 and HepG2-wt CM. These results suggest a role for VASH2 in the positive regulation of tube formation *in vitro* (Figures 6c and e). We obtained the similar results of Hep3B cells (Supplementary Figure 6S).

Taken together, these results demonstrate that VASH2-SVBP CM significantly increases the proliferation, migration and tube formation of HUVECs, whereas *VASH2*-knockdown HCC cells CM decreases these abilities of HUVECs, indicating that VASH2 has a direct effect on HUVEC cells via a paracrine mechanism.

VASH2 promotes tumor growth and angiogenesis *in vivo*

To further study the effects of VASH2 on HCC proliferation and angiogenesis, *in vivo* experiments were performed via the subcutaneous transplantation of transduced cells into BALB/cA-nu nude mice. After injection, we measured the size of the growing tumors every 4 days for 20 days, after which the mice were euthanized. The tumor sizes of the HepG2-shVASH2 group were significantly smaller than the HepG2-VASH2 and HepG2-wt groups (Figure 7a). Growth curves of the tumors were also generated, and we found that after 16 days, the tumors of the *VASH2*-knockdown group were significantly smaller (Figure 7b). This *in vivo* result is consistent with the *in vitro* studies. The tumors were excised, and RNA was extracted to confirm that the stable transduction of *VASH2* was maintained (Figure 7c). Immunohistochemical analysis using frozen sections of the tumors and a CD31-specific antibody

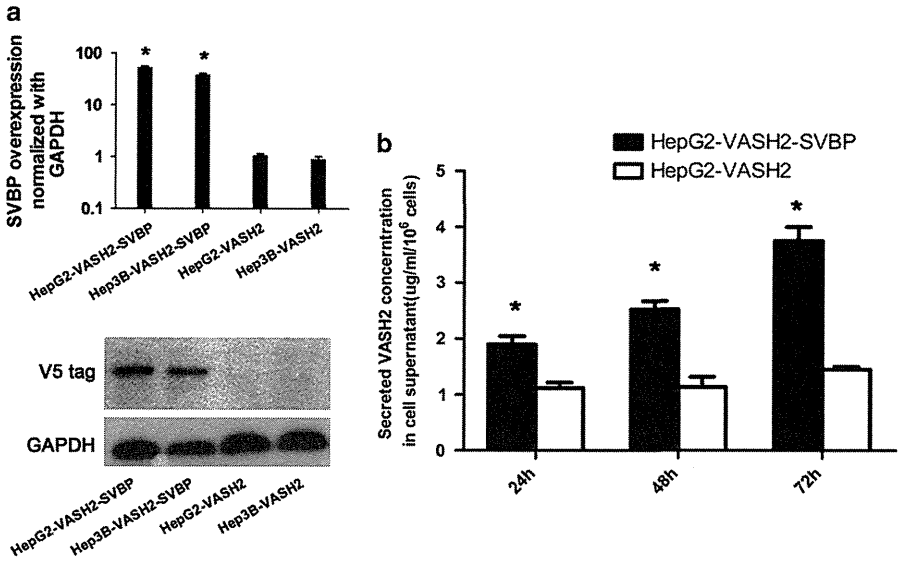

Figure 5. SVBP facilitates VASH2 secretion in HCC cells by functioning as a chaperone. (**a**) SVBP was transfected in HepG2-VASH2 and Hep3B-VASH2 cells. qRT–PCR and western blot was used to measure the transfection efficiency. V5 tag was fused with SVBP so that V5 antibody used as a substitute of SVBP antibody. (**b**) Overexpression of SVBP increases VASH2 secretion into the medium. VASH2 secretion was measured at three different time points using enzyme-linked immunosorbent assay assay. VASH2 secretion from HepG2-VASH2-SVBP cells was significantly higher than secretion from HepG2-VASH2 cells. Each group was tested in triplicate. $^*P<0.05$ when compared with the control group.

was performed to measure the microvessel density. Each slide was evaluated with three fields, and data were analyzed as mean vessel number of these three fields. The tumors from the HepG2-shVASH2 group contained significantly fewer microvessels (Figure 7d). Hep3B had the similar results to HepG2 (Supplementary Figure 7S).

In addition, we also confirmed the angiogenic effects of VASH2 on HCC *in vivo* using Matrigel plug assays. HepG2-VASH2, HepG2-wt and HepG2-shVASH2 cells were suspended in a Matrigel/Dulbecco's modified Eagle's medium (DMEM) mixture and subcutaneously injected into mice. Consistent with the previous results, the HepG2-shVASH2 cells formed significantly fewer vessels compared with the HepG2-VASH2 and HepG2-wt cells (Figure 8a). Furthermore, the hemoglobin concentration was measured following Matrigel dissolution. The HepG2-shVASH2 group also showed significantly lower levels of hemoglobin (Figure 8b, $P<0.05$). We had the similar results of Hep3B cells (Supplementary Figure 8S).

These data indicate that knockdown of *VASH2* significantly inhibits tumor growth and angiogenesis, indicating that VASH2 has a role in promoting HCC proliferation and angiogenesis. Interestingly, the HepG2-VASH2 group did not show greater tumor growth or angiogenesis than the HepG2-wt group. This might reflect the fact that wild-type HepG2 cells already have relatively high VASH2 expression or that enhancing angiogenesis via a paracrine mechanism is pivotal for VASH2 to affect tumor growth. Exogenous overexpression of *VASH2* did not alter its secretion because VASH2 expression does not alter SVBP expression.

VASH2 promotes angiogenesis through fibroblast growth factor (FGF)-2 and VEGF via autocrine and paracrine mechanisms

FGF-2 and VEGF are the most common angiogenic factors; therefore, we further explored whether VASH2 promoted angiogenesis through FGF-2 or VEGF. HepG2 cells expressing different levels of VASH2 and HUVECs were cocultured, and qRT–PCR was used to measure FGF-2, VEGF and VASH1 expression in the HepG2 cells and HUVECs. The HepG2-VASH2-SVBP cells, which secreted the most VASH2 increased FGF-2 (Figures 9a and b), VEGF (Figures 9c and d) and VASH1 (Figures 9e and f) expression both in the HepG2 cells and HUVECs ($^*P<0.05$ compared with HepG2-VASH2). In contrast, the HepG2-shVASH2 cells decreased FGF-2 (Figures 9a and b), VEGF (Figures 9c and d) and VASH1 (Figures 9e and f) expression at some of the time points ($\#P<0.05$ compared with HepG2-wt). This result indicates that secreted VASH2 might exert its effects on both HepG2 cells and HUVECs through autocrine and paracrine mechanisms. High levels of secreted VASH2 in HepG2-VASH2-SVBP cultures caused increases in FGF-2 and VEGF expression, which partly explains why VASH2 promoted angiogenesis *in vitro* and *in vivo*. At the same time, this suggests that SVBP is very important for VASH2 secretion. Interestingly, we also found that VASH1 expression was significantly increased, especially in HepG2-VASH2-SVBP cells, whereas other HepG2 cells had very low expression levels of VASH1. In addition, secreted VASH2 increased VASH1 expression in HUVECs. This phenomenon might give us a hint that there exists a dynamic balance of mutual restraint between angiogenic and anti-angiogenic factors. Increasing VASH2 may feedback to enhance VASH1 expression, similar to VEGF-mediated VASH1 upregulation.

DISCUSSION

Our studies demonstrate that *VASH2* is highly expressed in HCC cell lines and tissues and promotes HCC angiogenesis and malignant transformation. We also explored the mechanism underlying the transcriptional activation of *VASH2*. We analyzed the histone modifications present at the putative promoter of *VASH2*. Promoter activity was mainly localized to the −354 to −10 region, upstream of the TSS, and activating histone modifications (that is, increased H3K4triMe and H3Ac and decreased H3K27triMe) were found in this region, indicating that an epigenetic mechanism may be responsible for the increased *VASH2* expression in HCC. This epigenetic regulation pattern is very similar to that of the *Pax7* gene in satellite cells during muscle regeneration.[19] We hypothesized there may be a functional element located within the region −354 to −10, while histone modification facilitates this region for binding of trans factors, which deserves further investigation.

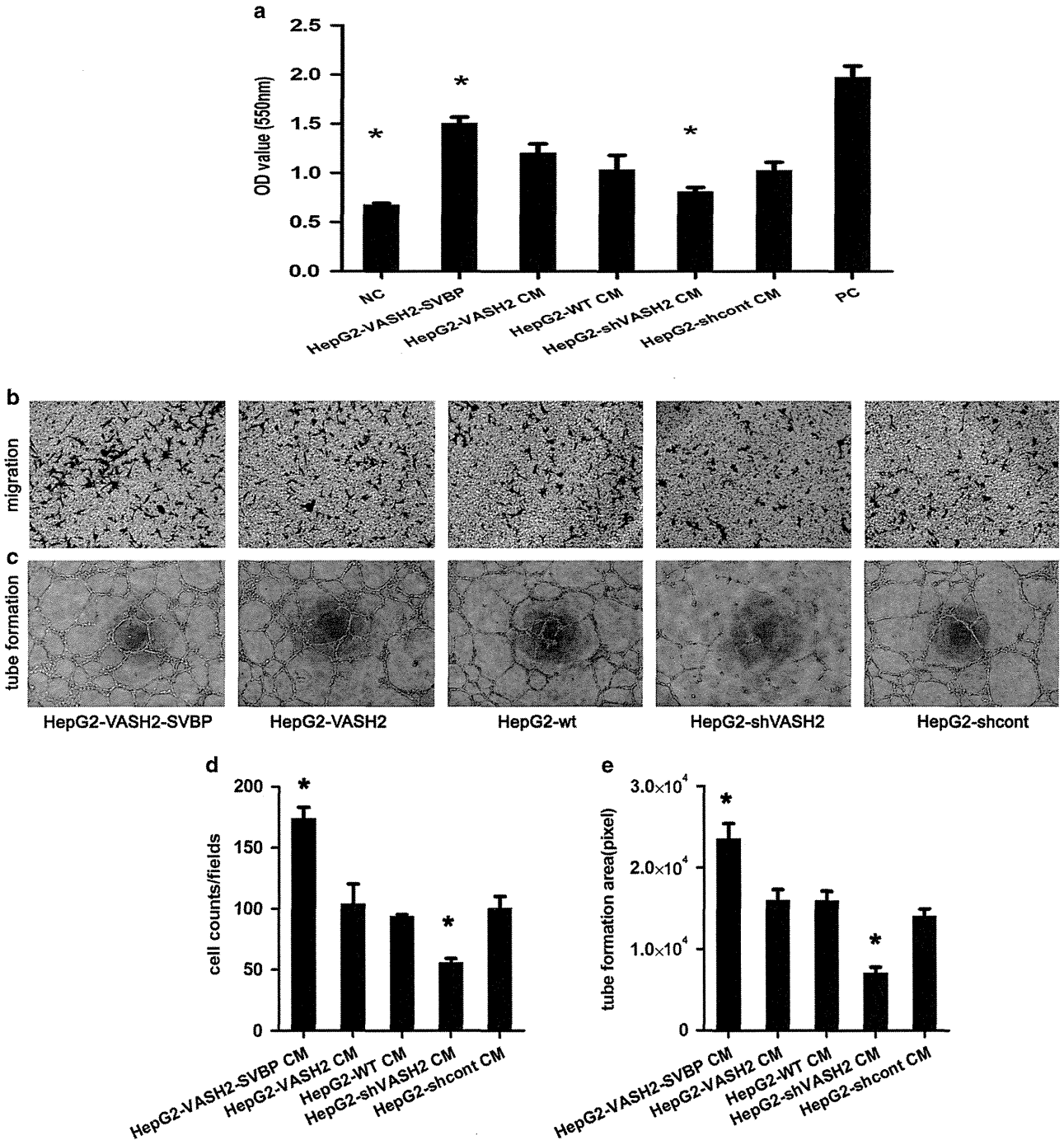

Figure 6. The effect of conditioned medium from different HepG2 cell lines on HUVECs. (**a**) Supernatant was collected from different HepG2 cell lines and added to HUVECs. 3-(4,5-Dimethythiazol-2-yl)-2,5-diphenyl tetrazolium bromide assay showed the HepG2-VASH2-SVBP CM promoted the proliferation of HUVECs more than the HepG2-VASH2 and HepG2-wt CM, whereas HepG2-shVASH2 decreased the proliferation of HUVECs compared with the control ($P<0.05$). The positive control (PC) was 10% fetal bovine serum–DMEM, and the negative control (NC) was DMEM. (**b**, **d**) A migration assay was performed. The lower chambers were seeded with various HepG2 cell lines, and the upper chambers were seeded with 10^4 HUVECs. The membranes of the chambers were stained with 0.1% Crystal violet, and four fields of each membrane were photographed and counted. (**c**, **e**) Tube formation assays. HUVECS (2×10^5 cells) were suspended in 100 μl CM and added to a Matrigel-coated surface. After 18 h, photos were taken and analyzed. *$P<0.05$. Each group was analyzed in triplicate, and the data are presented as the average ± s.d. A full color version of this figure is available at the *Oncogene* journal online.

VASH1, which is produced and secreted by vascular ECs, regulates EC proliferation and migration in an autocrine manner that is facilitated by SVBP. We found that supernatants from HepG2 cells have direct effects on HUVECs; therefore, we hypothesized that VASH2 requires from secretion to exert its effects. As VASH2 lacks a classic secretion signal sequence, we hypothesized that SVBP could function as a secretion chaperone for VASH2.

Similar to the results of Suzuki *et al.*,[18] we found constitutive expression of SVBP in HCC cells under basal conditions, and co-expression of SVBP increased VASH2 secretion. Therefore, the mechanism underlying VASH2 secretion might be the same as

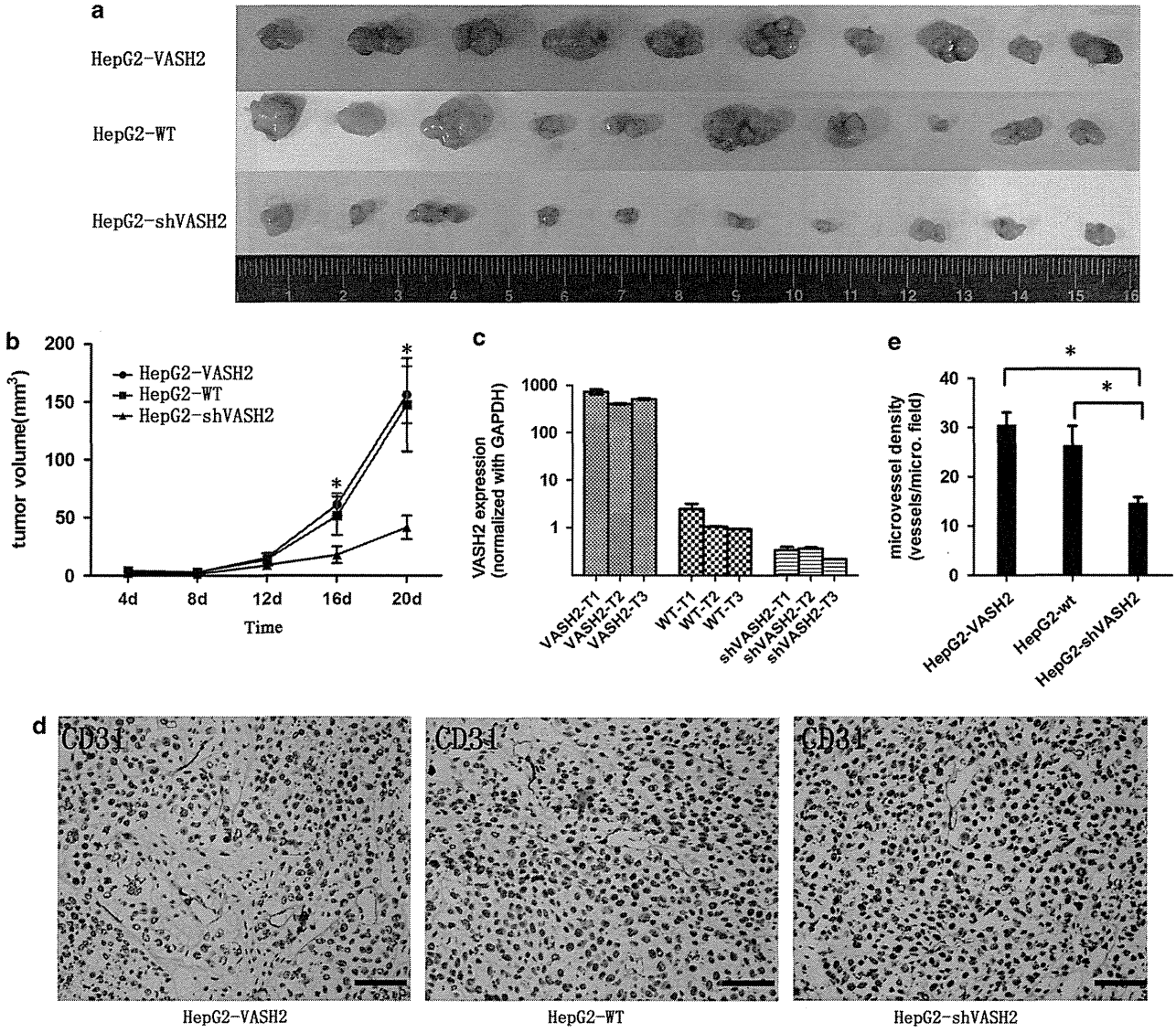

Figure 7. Subcutaneous injection of tumor cells. (**a**) HepG2-VASH2, HepG2-wt or HepG2-shVASH2 cells were suspended at a density of 10^7 cells/ml, and 100 μl was bilaterally injected into the flank of nude mice ($n = 5$). After 20 days the tumors were removed. The tumorigenesis rate was 100% for each group. The HepG2-shVASH2 tumors were smaller than those of the other groups, whereas the size of the HepG2-VASH2 tumors was not significantly different than that of the HepG2-WT tumors. (**b**) Tumor growth curves. After injection with tumor cells, the length and width of tumors were measured using vernier calipers every 4 days. The volume of the tumors was calculated using the equation volume = 1/2 × length × width^2. The data are presented as the average ± s.d. of 10 tumors for each group. *A significant difference between the groups when compared with the HepG2-shVASH2 group ($P < 0.05$). (**c**) Three tumors from each group were resected, mRNA was extracted and VASH2 expression was measured using qRT–PCR. (**d**) CD31 immunohistochemistry was performed on the tumor tissue from the HepG2-VASH2, HepG2-WT and HepG2-shVASH2 groups. All scale bars represent 200 μm; magnification, × 20. (**e**) Microvessel density of CD31 immunohistochemistry. Each slide was evaluated with three fields, and data were analyzed as mean vessel number of these three fields.

that of VASH1: SVBP is prepared in advance and accumulates under or at the cell surface. Once VASH2 protein is available, it binds SVBP, which facilitates the secretion of VASH2. Interestingly, the expression of SVBP and that of VASH2 are independent of one another. Overexpression of VASH2 did not increase SVBP expression, which would, in turn, have helped to further enhance VASH2 secretion. This may partly explain why the overexpression groups in our study were similar to the HepG2-wt group. In addition, VASH2 secretion is increased ~twofold following overexpression of SVBP. This suggests another mechanism, such as a cell surface channel or another chaperone, may assist VASH2 secretion. In addition, recombinant human VASH2 protein failed to promote tube formation of HUVECs in our assay, which might be due to a lack of processing and secretion (data not shown).

We also found that, through autocrine and paracrine mechanisms, VASH2 enhanced the expression of FGF-2 and VEGF, which have direct angiogenic activity. This phenomenon may partly explain how VASH2 promotes angiogenesis. In addition, we found nuclear factor-κB was upregulated about 1.7 ± 0.25-fold in VASH2-overexpressing HCC cells. As nuclear factor-κB was reported to has a key role in angiogenesis by regulating transcription of angiogenic growth factors (such as VEGF and FGF),[20,21] we consider nuclear factor-κB signal may be the possible mechanisms of VASH2 to upregulate VEGF and FGF-2. At the same time, VASH1 is upregulated following VASH2 overexpression

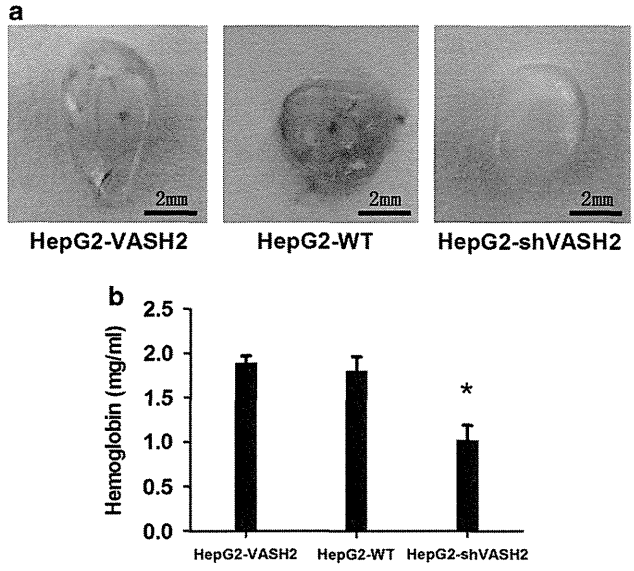

Figure 8. Matrigel plug assay. (**a**) Cells were suspended in Matrigel and DMEM and subcutaneously injected into the flanks of mice ($n=3$). After 15 days, the Matrigel plugs were removed and photographed. Representative Matrigel plugs from the HepG2-VASH2, HepG2-wt and HepG2-shVASH2 groups are shown. (**b**) The relative amount of angiogenesis was analyzed based on the RBC hemoglobin level, determined using the Drabkin method. The relative hemoglobin content is the hemoglobin level (mg) divided by the final volume of each plug. The data are presented as the mean ± s.d. for each group. *A significant difference when compared with the HepG2-shVASH2 group ($P<0.05$).

in HCC. This may be because angiogenic and anti-angiogenic factors are simultaneously activated during angiogenesis. However, the activity of the angiogenic factors is stronger than that of the anti-angiogenic factors. Our results are consistent with this hypothesis.

HCC, the most common primary liver tumor, relies on the formation of new blood vessels for growth. VEGF is critical for angiogenesis,[22,23] which has provided a strong rationale for anti-VEGF therapies.[5] However, the clinical use of VEGF inhibitors is more challenging than anticipated. Tumor angiogenesis can become VEGF-independent or even resistant to VEGF at more advanced stages because of the production of other angiogenic molecules.[24,25] In addition, anti-VEGF therapy has toxic vascular side effects such as proteinuria. In contrast with VEGF, VASH1, as a counter to VASH2, has been shown to both inhibit EC angiogenesis and protect EC from apoptosis. As a VEGF-independent and EC-extrinsic angiogenic factor, VASH2 is a novel target for anti-angiogenesis therapy.

In addition, VASH2 has been found to promote HCC cell proliferation in addition to angiogenesis. Therefore, VASH2 may exert other functions, such as invasion, which requires further study. Here, we mainly show the effects of VASH2 on HCC cells, we also have observed similar results in pancreatic cancer cells, indicating that VASH2 may function as an important tumor-associated gene in various solid tumors.

MATERIALS AND METHODS

HCC samples

Paired samples of cancerous liver tissue and adjacent non-cancerous liver tissue were obtained from 65 patients with HCC who underwent surgical resection at two centers (Jiangsu Province Hospital, China and Aichi Cancer Center Hospital, Nagoya, Japan) in accordance with the institutional policy. All patients provided written informed consent. In addition, samples of normal liver tissue were obtained from five patients who underwent a partial hepatectomy for liver metastasis of primary colon cancer. Tissue samples were flash frozen and stored at −80 °C.

Cell culture

Cells were maintained in DMEM (Gibco, 12100-046, Invitrogen, Carlsbad, CA, USA) containing 10% fetal bovine serum (Gibco, C2027-050, Uruguay), 100 mg/ml penicillin and 100 mg/ml streptomycin (Gibco, 15140122, Grand Island, NY, USA) at 37 °C with 5% CO_2. Human liver cancer cells HepG2 and Hep3B were obtained from the American Type Tissue Culture Collection (Manassas, VA, USA). Huh7 and L02 cells were provided by Professor Beicheng Sun of the Department of General Surgery, The First Affiliated Hospital of Nanjing Medical University (Nanjing, China). HUVECs were purchased from KeyGEN in China (KG110, Nanjing, China).

Plasmid construction and lentivirus packaging

VASH2 and *SVBP* lentiviral constructs were generated using PrimeSTAR HS DNA Polymerase (Takara, DR010A, Dalian, China) and the Lv-CMV-EGFP vector (the *SVBP* gene was fused with a V5 tag so that the V5 antibody could be used to measure VASH2 protein). shRNAs for human *VASH2* were designed in our lab and constructed in pLKO.1-puro vectors. Three shRNA plasmids (sh1, sh2 and sh3) were constructed against different *VASH2* targets, including a scrambled sequence as a negative control. All plasmids were verified by sequencing (Invitrogen). After infection with lentivirus, cells were tested for overexpression or knockdown of the *VASH2* gene. For knockdown, one construct (sh2), with ⩾85% knockdown efficiency, was used for further studies. The shRNA sequences used for further studies were as follows: shVASH2, 5′-CCGGTTTGACTTTGAGGACTCTTACCTCGAGGT AAGAGTCCTCAAAGTCAAATTTTTG-3′ and shScramble, 5′-CCGGCCTAAGGT TAAGTCGCCCTCGCTCGAGCGAGGGCGACTTAACCTTAGGTTTTTG-3′.

Quantitative RT–PCR

Total RNA was extracted from cells and tissues using TRIzol reagent (Invitrogen, 15596-026), and cDNA was synthesized using Primescript RT Reagent (TAKARA). qRT–PCR was performed on a 7500 Real-Time–PCR System (Applied Biosystems, Carlsbad, CA, USA) using Taqman probes for *GAPDH* (Hs99999.m1, Applied Biosystems) and *VASH2* (Hs00226928.m1). *GAPDH* was used as a reference to obtain the relative fold change for targets using the comparative Ct method.

Growth, cell cycle and apoptosis analysis

Cell growth was measured using a modified 3-(4,5–dimethythiazol–2–yl)-2,5-diphenyl tetrazolium bromide assay. Five groups of cells in logarithmic growth were seeded into 96-well plates. Each group was seeded in five duplicates. The cells were then cultured for 24, 48, 72, 96 or 120 h. Finally, the absorbance was measured using a microtiter plate reader (Tecan, Salzburg, Austria) with the 550 nm measuring wavelength and 620 nm reference wavelength. The growth of each group was calculated by averaging the optical density.

Cell cycle and apoptosis were performed as previously described by flow cytometry (Becton Dickinson, San Jose, CA, USA)[26]

Tube formation

HepG2-VASH2-SVBP, HepG2-VASH2, HepG2-wt, HepG2-shVASH2 and HepG2-shcont cells were cultured as described above. When the cells reached 80% confluence, the culture medium was changed to DMEM without fetal bovine serum. After an additional 48 h culture, the supernatant was collected as CM and stored at −20 °C. After thawed at 4 °C overnight, the Matrigel (BD, 356230, Bedford, MA, USA) was coated in 96-well plate then incubated at room temperature for at least 30 min to gel. HUVECs were suspended at a density of 2×10^5 cells/ml in the different CMs. The cell suspensions (100 μl) were added to each Matrigel-coated well. DMEM was substituted for CM for the negative control. After 18 h, the formed networks were photographed and analyzed using Image-Pro Plus (Media Cybernetics, Bethesda, MD, USA) to calculate the area of network as described previously.[27]

In vivo tumorigenesis experiments

Four-week-old male nude mice (BALB/cA-nu (nu/nu)) were purchased from the Shanghai Experimental Animal Center (Chinese Academy of Sciences, Shanghai, China). A total of 15 mice were randomly divided into three groups. HepG2-VASH2, HepG2-wt and HepG2-shVASH2 cells were

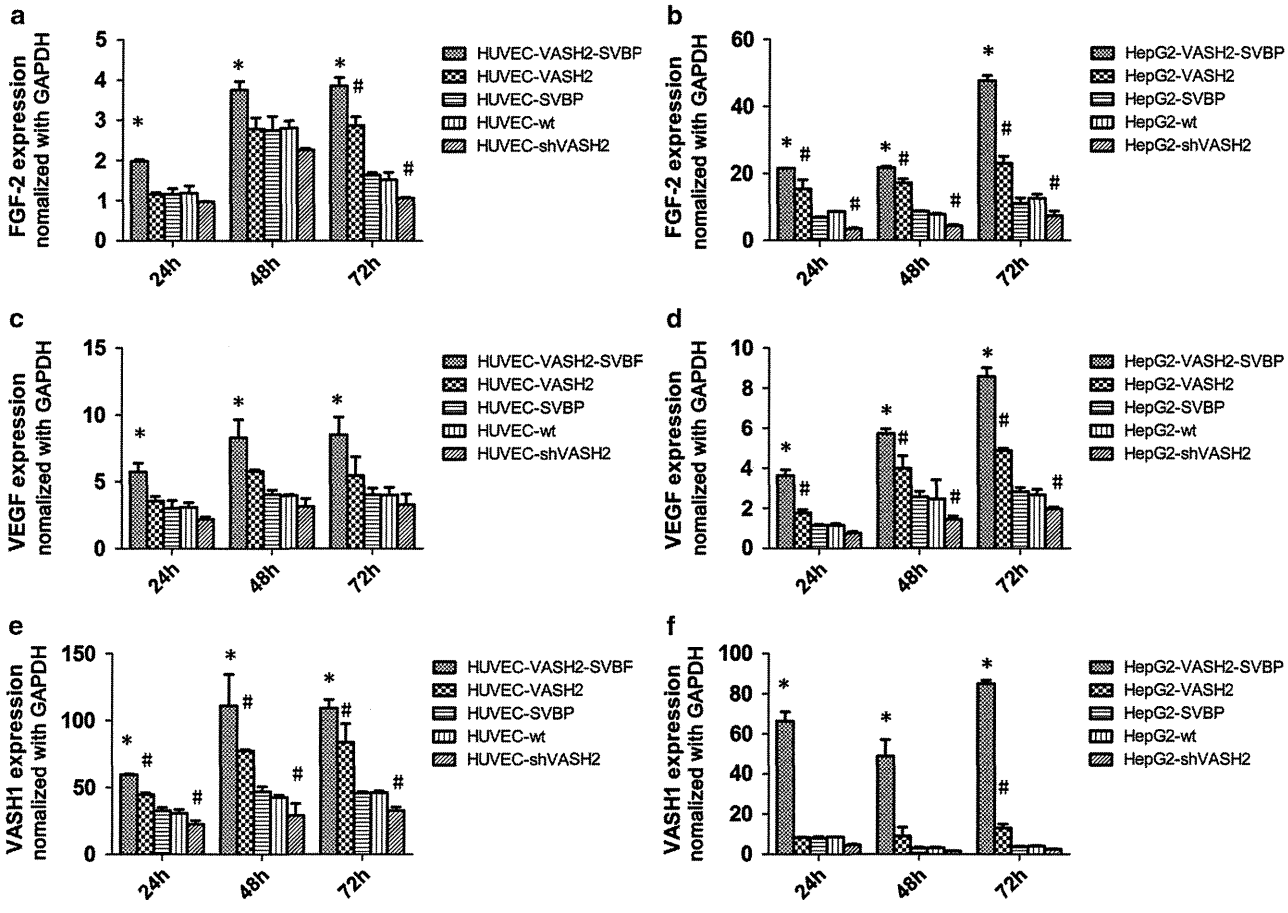

Figure 9. Expression of VASH2 with or without SVBP co-expression. VASH2 regulates the expression of FGF-2, VEGF and VASH1 in HUVECs and HepG2 cells in a coculture system. HepG2-VASH2-SVBP cells secreted the most VASH2 and increased the level of FGF-2 (**a**, **b**), VEGF (**c**, **d**) and VASH1 (**e**, **f**) both in HepG2 cells and HUVECs ($^{*}P<0.05$ when compared with HepG2-VASH2). HepG2-shVASH2 CM decreased FGF-2 (**a**, **b**), VEGF (**c**, **d**) and VASH1 (**e**, **f**) expression at some time points ($^{\#}P<0.05$ when compared with HepG2-wt).

bilaterally injected subcutaneously into the flanks of the mice (10^6 cells/100 μl per flank). Bidimensional tumor measurements were taken with calipers every 4 days, and the mice were euthanized after 20 days. The tumor volume was calculated using the formula (width^2 × length)/2.

Matrigel plug angiogenesis assay

Nine male mice were randomly divided into three groups. HepG2-VASH2, HepG2-wt and HepG2-shVASH2 cells were resuspended at 5×10^7 cells/ml in serum-free medium. Aliquots of cells (0.1 ml, 5×10^6 cells) were mixed with 0.4 ml Matrigel and bilaterally injected into the flanks of each mouse (100 μl cell mixture/per flank). Matrigel mixed with medium alone was used as a negative control. The Matrigel plugs were removed 15 days after implantation and used for the measurement of hemoglobin content using Drabkin's reagent (Sigma, D5941, St Louis, MO, USA). The data are presented as the mean ± s.d. from replicate experiments.[28]

Immunohistology and microvessel density analysis

Frozen tissue sections were fixed in acetone and methanol (1:1) for 10 min and were then rinsed. After blocking endogenous peroxides and proteins, slides were incubated with diluted rat-anti-mouse CD31 antibody (BD Pharmingen, 550274, Franklin Lakes, NJ, USA) for 2 h at 37 °C then incubated with horseradish peroxidase–conjugated goat-anti-rat secondary antibody (Santa Cruz, sc-2032, Santa Cruz, CA, USA) for 1 h at 37 °C, incubated with a 3,3′-diaminobenzidine solution for 10 min and counterstained with hematoxylin.

Staining against the endothelial marker CD31 by means of immunohistochemistry was followed by observation under low magnification scope (× 10). Tumor slides were examined in a blinded manner and representative areas of vital tumor were selected for examination. Each slide was evaluated with three fields, and data were analyzed as mean vessel number of these three fields.[29]

Western blot

Cell lysates were prepared by extracting protein with radioimmuno precipitation assay buffer. Membranes were blocked in 5% non-fat dried milk and incubated overnight at 4 °C with appropriate primary antibodies (the mouse-anti-human VASH2 monoantibody utilized in western blot was described previously[11]). GAPDH (AG019-1, Beyotime, Nantong, China)).

Dual luciferase reporter assay

Overlapping segments surrounding the TSS of the *VASH2* gene were amplified and ligated into the pGL3 basic vector. The plasmids were co-transfected with the *Renilla* luciferase expression plasmid into HepG2 cells. After 48 h, cells were collected and luciferase activity was measured using the Dual Luciferase Reporter Assay System (Promega, E1910, Madison, WI, USA). The relative promoter activity was calculated as firefly fluorescence/*Renilla* fluorescence.

Chromatin immunoprecipitation

We carried out a ChIP assay according to instructions from Upstate Biotechnology. The following antibodies were used as follows: anti-trimethyl-histone H3 (lys4) antibody (07-473, Upstate Biotechnology, Lake Placid, NY, USA), anti-trimethyl-histone H3 (lys27) antibody (17–622, Upstate) and anti-acetyl-histoneH3 antibody (17–615, Upstate). Normal rabbit immunoglobulin G was used as a 'no antibody' control. Real-time–PCR was performed with SYBR Premix EX Taq (Takara). The amount of immunoprecipitated DNA was normalized to the input DNA as the following formula: $\Delta Ct_{(normalized\ ChIP)} = (Ct_{(ChIP)} - (Ct_{(Input)}\text{-Log2 (input dilution factor)}))$, $\%Input = 2^{(-\Delta Ct(normalized\ ChIP))}$. Average relative amount of